BIOLOGY OF THE RED ABALONE, HALIOTIS RUFESCENS, IN NORTHERN CALIFORNIA

A Thesis

Presented to

The Faculty of the Department of Marine Science

San Jose State University

In Partial Fulfillment

of the Requirements for the Degree

Master of Science

by

Robert Thomas Leaf

December 2005

ABSTRACT

BIOLOGY OF THE RED ABALONE, HALIOTIS RUFESCENS, IN NORTHERN CALIFORNIA

By Robert Thomas Leaf

The red abalone, Haliotis rufescens Swainson 1822, supports the only recreational free-dive abalone fishery in the United States. I examined annual survivorship of three size classes (< 100 mm, 100.1 to 178 mm, and > 178 mm) of red abalone from five sites in northern California and one site in southern California using capture-mark-recapture data. Survival was variable spatially and among size classes. Survivorship values were incorporated into a size based projection matrix model. Elasticity values were found to be greatest for the sub-legal red abalone 150 mm to 178 mm (maximum shell length) indicating that changes in the vital rates of this size class are most important to population growth. Current methods to describe the age-at-length relationship of red abalone are insufficient because shell lengths exceed those predicted by growth models. I evaluated the utility of analyzing atomic bomb generated radioisotope ^{14}C in shell to validate this relationship.

ACKNOWLEDGEMENTS

This work has been made by possible by the support and assistance of numerous people and organizations. First and foremost I would like to thank California SeaGrant Program # R/CZ-69PD TR, The American Museum of Natural History Lerner-Gray Fund for Marine Research, and the Dr. Earl H. Myers and Ethel M. Myers Oceanographic and Marine Biology Trust. Each provided research funding, without which this work would not have been possible. Because of the variety of aspects of population biology addressed in this work a diverse group of people were responsible for the improvement and completion of each section. I would especially like to thank Dr. Henry Mollet, Dr. Tom Ebert, and Dr. Laura Rogers-Bennett who were invaluable for the matrix population modeling work. Dr. Tomo Eguchi provided help in the construction and selection of survivorship models. Pete Haaker very generously let me evaluate his data from southern California. Dr. Greg Cailliet, Lisa Kerr, and Allen Andrews provided the impetus and enthusiasm to carry out radiocarbon sampling. I have been fortunate to have two homes during my time at Moss Landing, the Ichthyology and Benthic Labs. Both contributed to my graduate education immensely. Aaron Carlisle, Wade Smith, and Chris Rinewalt in the Ichthyology Lab and Aroon Melwani, Rhea Sanders, Linda Kuhnz, Peter Slattery, Dr. Stacy Kim, Jim Oakden, Dr. John Oliver, Kamille Hammerstrom , and Andrew Thurber in the Benthic Lab provided support, encouragement, and a place to call home throughout my graduate education. The wonderful community at Moss Landing, especially Gail Johnston, Donna Kline, Joan Parker and all of the library staff went beyond the call duty

to expedite the completion of this project. I am especially indebted to Dr. Greg Cailliet who has been supportive of my myriad of thesis proposals and provided my first introduction to population and fishery biology. He has provided support for this project and encouragement to pursue future graduate work. I would not have done either without his council and support. Dr. Laura Rogers-Bennett provided the opportunity to work on abalone through a SeaGrant traineeship. She is a generous pioneer in abalone biology and allowed me the use of her and California Department of Fish and Game data. I cannot thank her enough for the support and mentoring provided to me for the duration of this project. Dr. Jon Geller generously became a member of my committee and I very much appreciate his comments and suggestions of my manuscript. It was greatly improved by his efforts. In addition to the institutional support I received I have been extremely fortunate to have the indefatigable support of my family: Sierra, my Mom, Tony, and Scott.

TABLE OF CONTENTS

PAGE

PAGE

LIST OF TABLES

TABLE PAGE

CHAPTER 1

CHAPTER 2

TABLE PAGE

LIST OF FIGURES

FIGURE PAGE

CHAPTER 1

FIGURE PAGE

CHAPTER 2

CHAPTER 3

FIGURE PAGE

CHAPTER 1

Size-based annual survival probabilities for three size classes of red abalone, *Haliotis rufescens*, using mark-recapture data from northern and southern California

ABSTRACT

Size specific mortality rates are currently not available for northern California red abalone, *Haliotis rufescens*, the only recreational abalone fishery on the west coast. I examined annual survivorship of three size classes (< 100 mm, 100.1 to 178 mm, and > 178 mm) of red abalone from five sites in northern California and one site in southern California using capture-mark-recapture data. The number of tagged individuals (n = 273 to 2,145), census occasions (n = 3 to 7), and size composition of individuals (41.5 to 227 mm) were variable at each site. Four models were specified for each size class at each site and were analyzed using the Jolly-Seber-Cormack model. The annual survival probabilities of the smallest size class in the study (< 100 mm) at one site in northern California was 0.52 y^{-1} $\pm$ (0.05 SE) and was 0.36 y^{-1} $\pm$ (0.07 SE) to 0.51 y^{-1} $\pm$ (0.08 SE) in southern California. Annual survival probabilities of the median size class (100.1 to 178 mm) from four sites at northern California ranged from 0.47 y^{-1} $\pm$ (0.05 SE) to 0.71 y^{-1} $\pm$ (0.04 SE) and 0.55 y^{-1} $\pm$ (0.05 SE) to 0.83 y^{-1} $\pm$ (0.10 SE) in southern California. The largest size class designated in the study (>178 mm) had annual survivorship values of 0.26 y^{-1} $\pm$ (0.06 SE) to 0.95 y^{-1} $\pm$ (0.08 SE) in northern California and 0.42 y^{-1} $\pm$ (0.07 SE) to 0.76 y^{-1} $\pm$ (0.11 SE) in southern California. These results indicate that annual survival was variable temporally, spatially, and among size classes. This study is an example of how parsimonious models and conservative use of available data can allow survivorship estimates from previously unutilized capture-mark-recapture data. These results will be useful for managers to better sustain the northern California fishery.

INTRODUCTION

Red abalone, *Haliotis rufescens*, is historically the most important commercial species of abalone on the west coast of the United States and currently supports its only recreational abalone fishery (Cox 1960, Karpov *et al.* 2000). Concerns regarding the decline of red abalone stocks in California have led to a prohibition of commercial fishing throughout California and closure of recreational fishery south of San Francisco Bay in 1997. The recreational fishery in northern California is currently regulated through the use of gear restrictions, a minimum legal size limit (178 mm, maximum shell length), seasonal closures, and daily and annual bag limits (California Department of Fish and Game (CDFG), Marine Region 2005).

Vital rates, such as annual survival, are difficult to quantify for wild populations but are necessary for determination of conservation and fishery management strategies. The effectiveness of minimum size limits for red abalone have been investigated using egg per recruit (EPR) and yield per recruit (YPR) models of southern California populations (Tegner *et al.* 1989). The results of EPR and YPR analysis of red and pink abalone (*H. corrugata*) populations and blacklip abalone (*H. rubra*) are sensitive to changes in the estimated annual survival (Nash 1989, Tegner *et al.* 1989). Furthermore, elasticity analysis of a Lefkovitch matrix projection model of red and white abalone (*H. sorenseni*) revealed that elasticity values are also sensitive to changes in annual survivorship ($1 - e^{(M)}$), where M is the instantaneous rate of mortality (Rogers-Bennett and Leaf in press).

Few estimates of annual survivorship of red abalone exist for California populations. Tegner *et al.* (1989) used five years of length frequency distributions to estimate instantaneous natural mortality of adult red abalone in southern California. They estimated M = 0.15 (annual survival probability 0.86 y^{-1}). In central California, Hines and Pearse (1982) found that mortality of red abalone in central California varied from 0.3 to 1.0 (annual survival probability 0.74 y^{-1} to 0.36 y^{-1}). Estimates of size specific rates of survival are lacking for northern California red abalone populations.

Abalone mortality has been shown to vary with age and size (Shepherd and Breen 1992). Therefore, the use of survival rate estimates from central and southern California and one life stage may not be sufficient for management needs of northern California populations. Cormack (1964), Jolly (1965), and Seber (1965), developed algorithms to estimate survivorship of open populations based on capture-mark-recapture experiments. Survivorship and recapture estimates are made by specifying biologically meaningful *a priori* models, using tag-recapture data, performing goodness-of-fit (GOF) testing of data conform to model assumptions, parameter estimate by the specified *a priori* models, and selection of the best fit model(s) (Lebreton *et al.* 1992). In this study, I use capture-mark-recapture data from five sites in northern and one site in southern California to estimate size class specific annual survivorship rates of red abalone.

METHODS

Red abalone tagging and census surveys in northern California were performed by personnel from the CDFG and Humboldt State University and in southern California by the CDFG. Tagging was conducted at five sites in northern California: North Pt. Cabrillo Cove (NC) and South Pt. Cabrillo Cove (SC) (39.364º N, 123.830º W), Van Damme State Park (VD) (39.274º N, 123.791º W), Pt. Arena (PA) (39.269º N, 123.799º W), and Fort Ross State Park (FR) (38.512º N, 123.244º W) (Figure 1) from 1971 to 1978 (Schultz *et al.* unpublished manuscript 1980, Ault and DeMartini 1987). Each of these sites is open to fishing with the exception of NC, a reserve where recreational and commercial fishing is prohibited. Tagging in southern California was conducted from 1978 to 1984 and occurred at a single location; Johnsons Lee (JL), which was open to recreational and commercial fishing (Figure 1) (Haaker *et al.* 1998). Each of these sites is characterized by rock and boulder habitat with kelp canopies of Bull kelp (*Nereocystis luetkeana*) at the five northern California sites and Giant kelp (*Macrocystis pyrifera*) in southern California.

Abalone were collected by SCUBA divers, brought to vessels or shore, measured for maximum shell length (MSL), and tagged. Stainless steel tags were individually numbered and were attached with steel wire threaded through the two respiratory pores distal to the umbo. Tagged abalone were returned to the locations and habitats where they were collected.

Annual tagging and recapture surveys were conducted throughout the year in northern California and July at Johnsons Lee (Table 1). At each of the northern California sites recapture history data of tagged red abalone were removed from analysis (Table 2).

Tagged red abalone recovered between sampling periods were excluded from analysis because frequently it was not possible to determine the fate of an individual after the tag had been reported. Removal of these individuals also minimized the potential adverse physiological effects associated with multiple handling between census periods.

Individual abalone tag-recapture histories were converted to a binary format (Lebreton *et al.* 1992). Binary recapture histories were displayed as vectors which consist of ones and zeros; a one represents the initial capture and subsequent re-sighting or recapture and a zero represents an occasion where an individual was not tagged or if tagged was not re-sighted. For example individuals with recapture history vector "101" were tagged at occasion t_1, not seen but were alive at t_2, and were seen at t_3 (Burnham *et al.* 1987, Lebreton *et al.* 1992). The presentation of recapture histories in this way is the format of input for a variety of mark-recapture computer programs (Lebreton *et al.* 1992).

Recapture history data from each site was partitioned into three size groups based on maximum shell length: Those individuals < 100 mm (MSL), termed the "cryptic" members of the population, those 100 to 178 mm (MSL), the "emergent sub-legal" sized individuals, and those > 178 mm (MSL), the "emergent legal sized" individuals.

The recapture histories of each size class at each site was tested to determine if data conformed to model assumptions; homogeneity of recapture and survivorship (Burnham *et al.* 1987, Lebreton *et al.* 1992). To do this I used Release Tests 2 and 3 which are a series of linked chi-square contingency tables that are used to test the assumptions of the equality of the probability of recapture (Test 2) and survival (Test 3) (Burnham *et al.* 1987). Recapture histories from sites that failed Release goodness-of-fit tests were not analyzed.

Following the notation of White and Burnham (1999), a "global model" was specified in which survivorship (φ) and recapture (p) probabilities were time dependent ($\varphi_t p_t$). I specified three additional models for analysis of each size class at each site: both parameters constant in time ($\varphi . p .$), survival probability variable with time and recapture probability constant ($\varphi_t p .$), and survival probability constant and recapture probability variable in time ($\varphi . p_t$). Site specific recapture history data were analyzed by parametric re-sampling to assess data dispersion, termed the quasi-likelihood parameter, $\hat{c}$, of the global model ($\varphi_t p_t$). Inflated values of $\hat{c}$ reveals a lack of fit to assumptions of the Cormack (1964), Jolly (1965), and Seber (1965) model. Site specific values of $\hat{c}$ for each size class $\geq$ 4.0 are considered over-dispersed (Burnham and Anderson 1998) and were eliminated from analysis.

Candidate models from size classes with satisfactory global models and $\hat{c} < 4.0$ were examined using the "recaptures only" protocol in program MARK. This algorithm estimates annual survivorship and recapture probabilities by multi-modal maximum likelihood estimation. Numerical iteration is used to estimate the values of φ and p that maximize the likelihood of the observed recapture frequencies. Thus the estimates of φ and p, given their frequencies for a three capture study with recapture histories "101", "110", "111", and "100", can be calculated in the following way (B is defined as φp and $X_{\#\#\#}$ are the number of individuals with this recapture history):

$$L(\varphi,p) = X_{101}\ln(\varphi(1 - p)\, B) + X_{110}\ln(\varphi p\, (1 - B)) + X_{111}\ln(\varphi p\, B) + X_{100}\ln(\varphi p(1 - B))$$

Variances of recapture and survival parameters are derived from the shape of the curve at the maximum likelihood estimate called the profile likelihood confidence interval (White and Burnham 1999).

The fit of a candidate model to recapture history data were compared based on their Akaike information criteria (AIC) values (Burnham and Anderson 1998). AIC is an information index that is commonly used for model selection (Forster 2000). It balances the fit of a particular candidate model to the data and the parsimony of the model, in terms of the number of model parameters, K; AIC = -2log Likelihood + 2K. Recent developments in model selection allow the data dispersion, evaluated as $\hat{c}$, to be incorporated into selection criteria. Each data set was evaluated using the four specified models with the adjusted $\hat{c}$ value of their respective global model. If the value of $\hat{c}$ (global model deviance/mean of re-sampled model deviance) is greater than 1.0, the recapture histories are over-dispersed. The resulting information values are referred to as the QAIC, the Quasi-AIC, (White and Burnham 1999):

$$QAIC = -2\log \text{Likelihood}/\hat{c} + 2K + 2K(K + 1)/(n - K - 1)$$

(n is the effective sample size). QAIC was used to rank candidate models (Burnham and Anderson 1998). If competing models have QAIC values within 2.0 ($\Delta QAIC \leq 2.0$) the competing models are considered equivalent (Burnham and Anderson 1998). Weighted parameter estimates can be computed for those models whose information criteria values are similar. Parameter estimates are derived as weighted averages based on their QAIC values (Buckland *et al.* 1997).

RESULTS

Recapture histories of tagged individuals were removed from analysis at each of the northern California sites (Table 2). South Cabrillo Cove Point (SC) had the fewest number of individuals used for analysis although it initially had the greatest number of tagged individuals, and only 54.2 % of individuals initially tagged were retained for analysis. No recapture histories were removed from the Johnsons Lee (JL) data because no tags were reported between the annual sampling periods at this site (Table 2).

The size range of tagged red abalone varied at each site and in some cases it was not possible to analyze every size class (Table 2). No recapture histories for individuals < 100 mm were available at Van Damme State Park (VD). There were few recapture histories < 100 mm at Point Arena (PA) (n = 16) and Fort Ross (FR) (n = 33), precluding analysis of this size class at these sites (Figure 2). There were a sufficient number of individuals to analyze recapture history data for each size class at JL, NC, and SC (Figure 2).

Tagging and census efforts were temporally variable at the study sites in northern California (Table 2). SC was the most intensively sampled site; the occasions of tagging and census of individuals had the fewest days between occasions and the shortest census periods for each sampling occasion (Table 2). VD had the fewest number of tagged individuals, less than half of any other site. NC, VD, PA, and FR had approximately annual tagging and occasions although the number of census occasions varied for each site.

Recapture history data were eliminated from analysis of some size classes at some sites by goodness-of-fit and $\hat{c}$ criteria (Table 3). It was not possible to test recapture history data for the size class < 100 mm for GOF Test 3 due to sparse data. However, the data passed Test 2 satisfactorily. Size class 100 to 178 mm from NC passed Test 2 ($p < 0.05$) but failed Test 3 ($p > 0.05$). The $\hat{c}$ values were low at this site (1.04 to 1.17). It was not possible to test any size class of the South Cabrillo Cove (SC) data for Test 3 because of few numbers of recaptures of tagged individuals at this site (Table 2), however the large $\hat{c}$ value revealed lack of fit to model assumptions for the < 100 mm and 100 to 178 mm size classes. Only data from the > 178 mm size class had a $\hat{c}$ value less than 4.0 at this site. Recapture histories for this size class passed Release Test 2 but it was not possible to analyze data using Test 3 because of sparse data. Recapture history data of the > 178 mm size class at VD, PA, or FR could not be tested with Release GOF because of the few numbers of individuals recaptured. However, over-dispersion, $\hat{c}$, was evaluated for the recapture history data at these sites, each had moderate $\hat{c}$ values.

No single candidate model fit the recapture histories of each size class at each site. In most cases more than one model was equivalent (ΔQAIC > 2) to describe the observed data (Table 4). For each of the < 100 and > 178 mm size classes at NC the constant survivorship ($\varphi.$) model was selected (ΔQAIC > 2) over competing models. Recapture history data from the 100 to 178 mm size class supported three equivalent models ($\varphi.p_t$, $\varphi_t p.$ and $\varphi.p$). Analysis of recapture history data from the single size class (> 178 mm) from SC indicated a model with constant survival rate ($\varphi.$) provided the best fit. Two candidate models were supported by QAIC criteria ($\varphi.p_t$) and ($\varphi_t p.$) for VD in the 100 to 178 mm size

class. No single model candidate for PA (100 to 178 mm) was supported over competing models (ΔQAIC $\leq$ 1.72). Three models were equivalent (ΔQAIC $\leq$ 0.01) for the recapture history profiles (> 178 mm) at PA. No model fit was supported overwhelmingly for the recapture history profiles for FR for the two size classes examined; 100 to 178 mm (ΔAIC $\leq$ 1.93) and > 178 mm (ΔQAIC $\leq$ 0.61). The recapture histories profiles for the smallest size class, < 100 mm, favored three equivalent models (ΔQAIC $\leq$ 0.89) over a fourth at JL. Analysis of recapture profiles for the size classes 100 to 178 mm (ΔQAIC $\geq$ 5.42) and > 178 mm (ΔQAIC $\leq$ 4.65) both favored the models with time varying survival rates.

Survivorship Estimates

QAIC weighted annual survivorship estimates varied among size classes and sites (Figure 3a,b). The annual survivorship estimate of the < 100 mm size class at NC, the only estimate available for this size class in northern California, was 0.52 y^{-1} $\pm$ (0.05 SE). Recapture history data from four sites permitted determination of annual survival estimates for the 100 to 178 mm size class (NC, VD, PA, and FR) (Figure 3a). The average survival estimate at NC ranged from 0.67 y^{-1} $\pm$ (0.05 SE) to 0.71 y^{-1} $\pm$ (0.04 SE). Candidate models predicted lower annual survivorship estimates of red abalone at the other three sites; ranging from 0.47 y^{-1} $\pm$ (0.05 SE) to 0.63 y^{-1} $\pm$ (0.10 SE). Annual survivorship of the > 178 mm size class in northern California (NC, SC, PA, and FR) was the most variable of any size class (Figure 3a). Red abalone at South Pt. Cabrillo Cove (SC) had the greatest annual survivorship 0.95 y^{-1} $\pm$ (0.08 SE) while individuals at NC had annual survival of 0.71 y^{-1} $\pm$

(0.04 SE) and individuals at PA and FR had annual survival estimates ranged from 0.26 y^{-1} $\pm$ (0.0.5 SE) to 0.36 y^{-1} $\pm$ (0.05 SE).

Survivorship estimates of the recapture history profiles in southern California had a similar pattern of size specific survivorship as the sites in northern California and also exhibited within site variation in each size class (Figure 3b). Survivorship of individuals in the > 178 mm size class had similar but generally lower annual survivorship values; 0.41 y^{-1} $\pm$ (0.07 SE) to 0.76 $\pm$ y^{-1} (0.10 SE) to those in the median size class; 0.55 $\pm$ y^{-1} (0.05 SE) to 0.83 y^{-1} $\pm$ (0.10 SE) (Figure 3b). Individuals in the < 100 mm size class had estimated annual survivorship values of 0.37 y^{-1} $\pm$ (0.07 SE) to 0.50 y^{-1} $\pm$ (0.10 SE).

Total mortality was variable at the three sites for which it was possible to estimate survivorship of the > 178 mm size class. Average total mortality, fishing and natural mortality (Z), at FR and PA was 1.34 and 1.02. Individuals at SC, although subjected to fishing pressure, had greatly reduced mortality, Z = 0.05, for the > 178 mm size class. Natural mortality of legal sized individuals, M, at NC the fishing reserve ranged from 0.41 to 0.34.

Recapture Estimates

Recapture estimates varied temporally at some sites and among size classes. The best fit model for each of the size classes < 100 mm and > 178 mm at NC were those with constant recapture rates, *p*. (Figure 4a). Recapture rates for the 100 to 178 mm size class varied throughout the study period, 0.46 y^{-1} $\pm$ (0.05 SE) to 0.56 y^{-1} $\pm$ (0.04 SE). Recapture rates of the > 178 mm size class at SC and 100 mm to 178 mm at VD also varied

throughout the study period. Recapture estimates for the 100 to 178 mm size classes at PA and FR were lower than those at NC; 0.29 y^{-1} ($\pm$ 0.05 SE) to 0.51 y^{-1} ($\pm$ 0.13 SE). Estimates for recapture rates for individuals > 178 mm at FR and PA were similar: 0.51 y^{-1} ($\pm$ 0.13 SE) to 0.52 y^{-1} ($\pm$ 0.08 SE). Estimated recapture rates varied for the < 100 mm and 100 to 178 mm size classes in northern California. Individuals in the < 100 mm size class at NC had lower recapture rates, 0.37 y^{-1} ($\pm$ 0.06 SE) than individuals in the 100 to 178 mm and > 178 mm size class.

DISCUSSION

This study documents the variable nature of red abalone survivorship both spatially and between size classes. Red abalone survival estimates generally increased with increasing size but were heterogeneous temporally and between sites. Fishing mortality was also variable among sites. Size specific survivorship estimates are especially important for species, such as abalone, that are difficult to age or whose vital rates appear to be determined by size and not age.

The largest size class designated in the study, the "emergent" legal sized individuals (> 178 mm), are susceptible to direct and indirect fishing mortality. Individuals at the SC site had the greatest annual survivorship which was surprising because this site was open to recreational fishing during the course of the study. Emergent individuals at NC and SC had greater annual survival rates than individuals at PA and FR. The difference among survivorship estimates at these sites is likely due to fishing mortality. The difference in

mortality between PA and FR in comparison to SC and NC is M = 0.93 to 1.29. Both PA and FR are easily accessible to recreational divers, are generally shallow, and are relatively protected from NW swell. The unique topography of SC, which is characterized by large pinnacles that slope to deep depths (> 35 feet deep) may provide a depth refuge for tagged abalone > 178 mm. Total mortality at this SC most likely represents natural mortality with very light fishing pressure. NC is a reserve where fishing is not allowed and therefore the mortality (M = 0.34 to 0.41) represents mortality without fishing. Annual survival estimates from JL are variable annually and may be related to oceanic conditions and heterogeneous fishing pressure. The annual survivorship estimates of this study were similar to those found for adult, emergent red abalone by Hines and Pearse (1982) but are less than those estimated by Tegner *et al.* (1989).

Individuals of the "emergent sub-legal" size class (100 to 178 mm) may differ from those in the smaller size class because they reach a size refuge from benthic invertebrate predators and are excluded from some of the rock cobble and crevice habitat. Individuals in the emergent sub-legal size classes are visible to research divers and to recreational fishers. Although members of this size class are not subject to direct fishing mortality they are susceptible to incidental mortality in the form of "bar cuts" where recreational fishing is allowed. During fishing, sub-legal individuals may be removed from the substrate by recreational fishers but gauges show they are less than the legal size limit and must be returned.

It is possible that removal of individuals for tagging and subsequent measuring may be a source of tagging mortality although it is likely minimal. Mortality of red abalone

caused by the census of individuals in this study by experienced divers on SCUBA, who are not limited by dive time like a breath hold recreational fisher, is probably very low. No statistical difference in growth was found for tagged red abalone in southern California, JL, caught and released annually and those caught and released biennially (Haaker *et al.* 1998) indicating that experimental manipulation did not cause deleterious physiological effects.

Although the 100 to 178 mm size classes at each site failed Release test 2 and 3, $\hat{c}$ values were sufficiently small to justify the inclusion of these data in analysis. Burnham *et al.* (1987) have noted that failures of release tests are frequent in studies with releases of initially marked and previously marked individuals. In many studies experimenters perform or present no release tests (Koenig *et al.* 1998, Tucker *et al.* 2001, Mills *et al.* 2002, Doherty *et al.* 2004). In some cases this is because candidate models contain parameters that are associated with individual covariates or because the inclusion of the quasi-likelihood parameter into candidate models is considered sufficient if the recapture history data fails Release GOF (Connolly and Miller 2001, Dinsmore and Collazo 2003).

The emergent sub-legal size class at NC in northern California, the fishing reserve, had greater annual survival than individuals of this size class at the other sites with fishing. Differences in estimated survivorship between the reserve and fished sites may represent fishing mortality, site related differences, or may be a result of ad hoc size partitioning of recapture histories. The differences in the number of individuals of sizes within the 100 to 178 mm size class differed between sites (Figure 2). NC had a relatively uniform distribution of individuals within this size class. The composition of individual sizes at SC was skewed toward smaller individuals and the composition of individuals at VD and PA

are skewed toward larger individuals. The southern California site, JL, had comparable survivorship to NC but showed greater temporal variability.

Of the three size classes defined in this study the smallest size class, the cryptic members of the population, were the hardest to detect and were encountered on transects only by divers closely inspecting the substrate. These individuals were found at the smallest sizes as newly settled individuals in crustose coralline algae (Shepherd and Breen 1989) as well as among urchin spines (Rogers-Bennett and Pearse 2001) and in rock cobble habitat. Parameter estimates of survival for individuals in this size class were available for one site in northern California (NC) and the southern California site (JL). Although survival estimates at JL exhibited more variation than those at NC the estimates are similar and are low compared to individuals in the larger size classes.

The heterogeneity of recapture rates is indicative of the ecology of each size class and the variable effort expended at each study site. The size specific recapture rates at NC and JL reflect the difficulty of detecting small individuals because of their cryptic ecology and the ability of divers to detect them. Recapture rates of the larger size classes at VD, SC, FR, and PA are extremely variable and probably reflect the effort expended in recapturing tagged individuals. Heterogeneity of effort is especially true for VD and FR whose range of days of census were from ten to 100 and twelve to 68 days, respectively.

Studies such as this one and others that use previously unutilized mark and re-capture data have the potential to be useful in the estimation of vital rates (Langtimm *et al.* 1998). These authors have shown that unbiased retrospective analysis can be performed given consistent data collection and conservative criteria to censor data. In this study I

used GOF and $\hat{c}$ criteria to censor data and was conservative in the construction of a posteriori candidate models. These data from capture-mark-recapture experiments, previously used for determination of age and growth relationships, movement, and stage transition probabilities (Ault and DeMartini 1987, Haaker *et al.* 1998, Rogers-Bennett and Leaf in press) provide useful data for the description of size specific survivorship patterns of red abalone. These results are invaluable in the use of egg-per-recuit analysis, the current management tool for the fishery, and other conservation and fishery models.

LITERATURE CITED

Ault, J.S., and DeMartini, J.D. (1987). Movement and dispersion of red abalone, *Haliotis rufescens*, in northern California. California Fish and Game 73(4):196-213.

Buckland, S.T., Burnham, and N.H. Augustin. 1997. Model selection: an integral part of inference. Biometrics 53:603-618.

Burnham, K. P., Anderson, D. R., White, G. C., Brownie, C. and K. H. Pollock. 1987. Design and analysis methods for fish survival experiments based on release-recapture. American Fisheries Society Monograph 5.

Burnham, K.P. and D.R. Anderson. 1998. Model selection and inference: a practical information theoretical approach. Springer-Verlag, New York, New York

California Department of Fish and Game, Marine Region. 2005. Abalone Recovery and Management Plan. 359 pages. Available at: www.dfg.ca.gov/mrd/armp/entire.html

Connolly, S.R. and Miller, A.I. 2001. Joint estimation of sampling and turnover rates from fossil databases: Capture-mark-recapture methods revisited. Paleobiology 27:751-767.

Cormack, R.M. 1964. estimates of survival from the sighting of marked individuals. Biometrika 51:429-438.

Cox, K. W. 1960. Review of the abalone in California. California Fish and Game 46:381-406.

Dinsmore, S.J. and J.A. Collazo. 2003. The influence of body condition on local apparent survival of spring migrant sanderlings in coastal North Carolina. The Condor 105: 456-473.

Doherty, P.F., A. Schreiber, J.D. Nichols, J.E. Hines, W.A. Link, G.A. Schenk, and R.W. Schreiber. 2004. Testing life history predictions in a long-lived seabird: A poplation matrix approach with improved parameter estimation. Oikos 105:606-618.

Forster, M.R. 2000. Key Concepts in Model Selection: Performance and Generalizability. Journal of Mathematical Psychology 44:205-231.

Haaker, P.L., Parker, D.O., Barsky, K.C., and C.S.Y. Chun. 1998. Growth of red abalone, *Haliotis rufescens* (Swainson) at Johnsons Lee, Santa Rosa Island, California. Journal of Shellfish Research 17(3):747-753.

Hines, A.H. and J.S. Pearse. 1982. Abalones, shells, and sea otters: Dynamics of prey populations in central California. Ecology 63(5):1547-1560.

Jolly, G.M. 1965. Explicit estimates from capture-recapture data with both dead and immigration-stochastic model. Biometrika 52: 225-247.

Karpov, K.A., Haaker, P.L., Albin, D., Taniguchi, I.K., and D. Kushner. 1998. The red abalone, *Haliotis rufescens*, in California: Importance of depth refuge to abalone management. Journal of Shellfish Research 17:863-870.

Koenig, C.C. and F.C. Coleman. 1998. Absolute abundance and survival of juvenile gags in sea grass beds of the northeastern Gulf of Mexico. Transactions of the American Fisheries Society 127:44-55.

Langtimm, C.A., O'Shea, T.J., Pradel, R. and C.A Beck. 1998. Estimates of annual survival for adult Florida manatees (*Trichechus manatus latirostris*). Ecology 79:981-987.

Lebreton, J. D., K.P. Burnham, J. Colbert, and D.R. Anderson 1992. Modeling survival and testing biological hypotheses using marked animals: A unified approach with case studies. Ecological Monographs 62:67-118.

Mills, K.H., Chalanchuk, S.M., and D.J. Allan. 2002. Abundance, annual survival, and recruitment of unexploited and exploited lake charr, *Salvelinus namaycush*, populations at the Experimental Lakes Area, northwestern Ontario. Environmental Biology of Fishes 64:281-292.

Nash, W.J. 1992. An evaluation of egg-per-recruit analysis as a means of assessing size limits for blacklip abalone (Haliotis rubra) in Tasmania. In: S.A. Shepherd, M.J Tegner, S.A. Guzmán del Próo (eds.) Abalone of the World: Biology Fisheries and Culture. Fishing News Books. Oxford, p. 318-338.

Rogers-Bennett and Leaf, R.T. In press. Elasticity analyses of size-based red and white abalone matrix models: Management and conservation in California. Ecological Applications.

Rogers-Bennett, L., Rogers, D.W., and S. Schultz. In preparation. Estimating growth and mortality parameters for red abalone (Haliotis rufescens) in northern California.

Schultz, S.A., Jow, J., and J. Gaibel. 1980. Growth rates and status of the resource, and fishery for red abalone in northern California. State of California, The Resources Agency, Department of Fish and Game. Unpublished manuscript. 31 pages.

Seber, G.A.F. 1965. A note on the multiple-recapture census. Biometrika 52:249-259.

Shepherd, S.A., and P.A. Breen. 1992. Mortality in abalone: Its estimation, variability, and causes. In: S.A. Shepherd, M.J Tegner, S.A. Guzmán del Próo (eds.) Abalone of the World: Biology Fisheries and Culture. Fishing News Books. Oxford, p. 276-304.

Tegner, M.J., Breen, P.A., and C.E. Lennert. 1989. Population biology of red abalones, *Haliotis rufescens*, in southern California and management of the red and pink, *H. corrugata*, abalone fisheries. Fishery Bulletin 87:313-339.

Tucker, A.D., Gibbons, J.W., and J.L. Greene. 2001. Estimates of adult survival and migration for diamondback terrapins: Conservation insight from local extirpation within a metapopulation. Canadian Journal of Zoology 79:2199-2209.

White, G.C. and K. P. Burnham. 1999. Program MARK: Survival estimation from populations of marked animals. Bird Study **46** Supplement, 120-138.

Table 1. Site-specific CMR (capture-mark-recapture) summary statistics for red abalone tagged and recaptured in northern and southern California at North Cabrillo Pt. Cove (NC), South Cabrillo Pt. Cove (SC), Van Damme State Park (VD), Point Arena (PA) and Fort Ross State Park (FR),and the one southern California site; Johnsons Lee (JL). $date_i$ is the median date of tagged red abalone caught at census period i, z_i is the number of abalone captured before census occasion i. m_i is the number or after census occasion i but not during the ith period, R_i is the number of tagged abalone released at occasion i, and mi is the number of tagged individuals captured at census occasion i.

		Census occasion (i)						
Site	CMR statistic	1	2	3	4	5	6	7
NC	$date_i$	5/2/71	4/14/72	4/6/73	3/24/74	4/16/75	4/24/76	4/23/77
	m_i		99	74	53	44	53	137
	z_i		24	36	29	23	25	0
	R_i	230	199	80	120	128	312	
	r_i	123	86	46	38	55	112	
SC	$date_i$	4/24/75	12/10/75	4/24/76	11/5/76	4/15/77		
	m_i		148	87	87	48		
	z_i		101	105	31	0		
	R_i	453	148	87	87			
	r_i	249	91	13	17			
VD	$date_i$	4/23/74	5/17/75	6/24/76	6/4/77			
	m_i		48	38	15			
	z_i		7	6	0			
	R_i	175	112	64				
	r_i	55	37	9				

Table 1. continued

Site	CMR statistic	Census occasion (*i*) 1	2	3	4	5	6	7
	m_i		157	100				
	z_i		63	0				
	R_i	811	157					
	r_i	220	37					
FR	$date_i$	8/30/75	6/25/76	6/15/77				
	m_i		184	86				
	z_i		42	0				
	R_i	797	186					
	r_i	226	44					
JL	$date_i$	7/31/78	7/31/79	7/31/80	7/31/81	7/31/82	7/31/84	
	m_i		158	112	275	409	138	
	z_i		47	88	65	79	0	
	R_i	510	494	651	1032	412		
	r_i	205	153	252	423	59		

Table 2. Characteristics of red abalone study populations for the five northern California sites; North Cabrillo Pt. Cove (NC), South Cabrillo Pt. Cove (SC), Van Damme State Park (VD), Point Arena (PA) and Fort Ross State Park (FR), and one southern California site; Johnsons Lee (JL).

Site	minimum size (mm)	maximum size (mm)	Number of census occasions	Number of days for each census	Number of days between census occasions	Number of individuals tagged	Number of individuals for CMR analysis	Duration of tagging
NC	41.5	227	7	2 to 38	350 to 398	831	746	1971 to 1977
SC	53.5	208	5	1 to 13	135 to 237	836	453	1975 to 1977
VD	100.5	217	4	10 to 100	332 to 394	308	273	1974 to 1977
PA	71	217	3	3 to 40	354	811	786	1975 to 1977
FR	85	221	3	12 to 68	321 to 362	831	799	1975 to 1977
JL	55.5	222	5	1 to 30	364 to 350	2145	2145	1978 to 1984

Table 3. Summary of goodness-of-fit (GOF) tests and binomial dipersion (*c_hat*) values of recapture history data for size partitioned recapture history data at each site. Test 2 and Test 3 are those of Program Release (Burnham et al. 1987). *c_hat* values are calculated as (global model deviance/mean of resampled model deviance).

Site	Size class (mm)	Test 2			Test 3			Test 2 + Test 3			
		X^2	df	p	X^2	df	p	X^2	df	p	*c_hat*
NC	< 100	3.405	4	0.493	-	-	-	-	-	-	1.05
	100 to 178	14.136	8	0.078	25.929	8	0.001	40.066	16	0.001	1.17
	> 178	1.968	4	0.742	4.233	7	0.753	6.202	11	0.860	1.04
SC	< 100	6.779	2	0.034	-	-	-	-	-	-	4.07
	100 to 178	1.283	3	0.733	-	-	-	-	-	-	5.61
	> 178	0.263	2	0.877	-	-	-	-	-	-	1.22
VD	100 to 178	2.708	1	0.100	0.979	3	0.806	3.686	4	0.450	1.06
	> 178	0	1	1.000	-	-	-	-	-	-	1.51
PA	100 to 178	-	-	-	-	-	-	-	-	-	1.00
	> 178	-	-	-	-	-	-	-	-	-	1.00
FR	100 to 178	-	-	-	-	-	-	-	-	-	1.13
	> 178	-	-	-	-	-	-	-	-	-	1.00
JL	< 100	0.872	3	0.832	1.647	5	0.863	2.774	8	0.948	1.52
	100 to 178	9.876	5	0.079	21.195	7	0.004	31.071	12	0.002	1.41
	> 178	0.415	3	0.937	2.698	7	0.912	3.113	10	0.979	1.45

Table 4. Model selection table of recapture history data from each site with *c_hat* values less than 3.0 and non-significant Release goodness-of-fit values. Recapture history data from NC (100 to 178 mm) and JL (100 to 178 mm) failed Test 3 but were included in CMR analysis. Candidate models for each size class in each site are in order of descending QAIC value.

Site	Size class (mm)	Number of individuals	Model	Number of parameters	QAIC	delta QAIC	QAIC weight
NC	< 100	179	$\cdot\, p_{\cdot}$	2	355.55	0	0.72
			$\cdot\, p_{t}$	7	357.76	2.2	0.24
			$_{t}p_{\cdot}$	7	361.44	5.88	0.04
			$_{t}p_{t}$	11	365.32	9.77	0.01
NC	100 to 178	470	$\cdot\, p_{\cdot}$	2	1131.51	0	0.40
			$\cdot\, p_{t}$	7	1131.57	0.06	0.39
			$_{t}p_{\cdot}$	7	1133.35	1.83	0.16
			$_{t}p_{t}$	11	1136.07	4.56	0.04
NC	> 178	97	$\cdot\, p_{\cdot}$	2	261.13	0	0.91
			$_{t}p_{\cdot}$	7	266.78	5.65	0.05
			$\cdot\, p_{t}$	7	267.96	6.83	0.03
			$_{t}p_{t}$	11	271.03	9.9	0.01
SC	> 178	24	$\cdot\, p_{t}$	5	97.83	0	0.66
			$\cdot\, p_{\cdot}$	2	100.78	2.95	0.15
			$_{t}p_{\cdot}$	5	101.03	3.2	0.13
			$_{t}p_{t}$	7	102.73	4.9	0.06
VD	100 to 178	166	$\cdot\, p_{t}$	4	307.79	0	0.39
			$_{t}p_{\cdot}$	4	307.90	0.11	0.37
			$_{t}p_{t}$	5	309.87	2.08	0.14
			$\cdot\, p_{\cdot}$	2	310.33	2.54	0.11
PA	100 to 178	558	$\cdot\, p_{\cdot}$	2	927.62	0	0.44
			$\cdot\, p_{t}$	3	929.34	1.72	0.19
			$_{t}p_{\cdot}$	3	929.34	1.72	0.19
			$_{t}p_{t}$	3	929.34	1.72	0.19
PA	> 178	238	$_{t}p_{\cdot}$	3	415.13	0	0.32
			$_{t}p_{t}$	3	415.13	0	0.32
			$\cdot\, p_{t}$	3	415.14	0.01	0.32
			$\cdot\, p_{\cdot}$	2	420.07	4.93	0.03

Table 4 continued

Site	Size class (mm)	Number of individuals	Model	Number of parameters	QAIC	delta QAIC	QAIC weight
FR	100 to 178	545	$\Phi_{.}\ p_{.}$	2	1017.65	0	0.47
			$\Phi_{.}\ p_{t}$	3	1019.58	1.93	0.18
			$\Phi_{t}\ p_{.}$	3	1019.58	1.93	0.18
			$\Phi_{t}\ p_{t}$	3	1019.58	1.93	0.18
FR	> 178	221	$\Phi_{.}\ p_{.}$	2	279.05	0	0.31
			$\Phi_{.}\ p_{t}$	3	279.66	0.61	0.23
			$\Phi_{t}\ p_{.}$	3	279.66	0.61	0.23
			$\Phi_{t}\ p_{t}$	3	279.66	0.61	0.23
JL	< 100	336	$\Phi_{t}\ p_{.}$	6	347.16	0	0.38
			$\Phi_{.}\ p_{.}$	2	347.36	0.21	0.35
			$\Phi_{.}\ p_{t}$	6	348.05	0.89	0.25
			$\Phi_{t}\ p_{t}$	9	352.81	5.65	0.02
JL	100 to 178	1390	$\Phi_{t}\ p_{t}$	9	2596.37	0	0.94
			$\Phi_{.}\ p_{t}$	6	2601.79	5.42	0.06
			$\Phi_{t}\ p_{.}$	6	2620.68	24.32	0.00
			$\Phi_{.}\ p_{.}$	2	2629.31	32.95	0.00
JL	> 178	419	$\Phi_{t}\ p_{.}$	6	638.38	0	0.81
			$\Phi_{.}\ p_{t}$	6	643.03	4.65	0.08
			$\Phi_{t}\ p_{t}$	9	643.06	4.68	0.08
			$\Phi_{.}\ p_{.}$	2	645.20	6.81	0.03

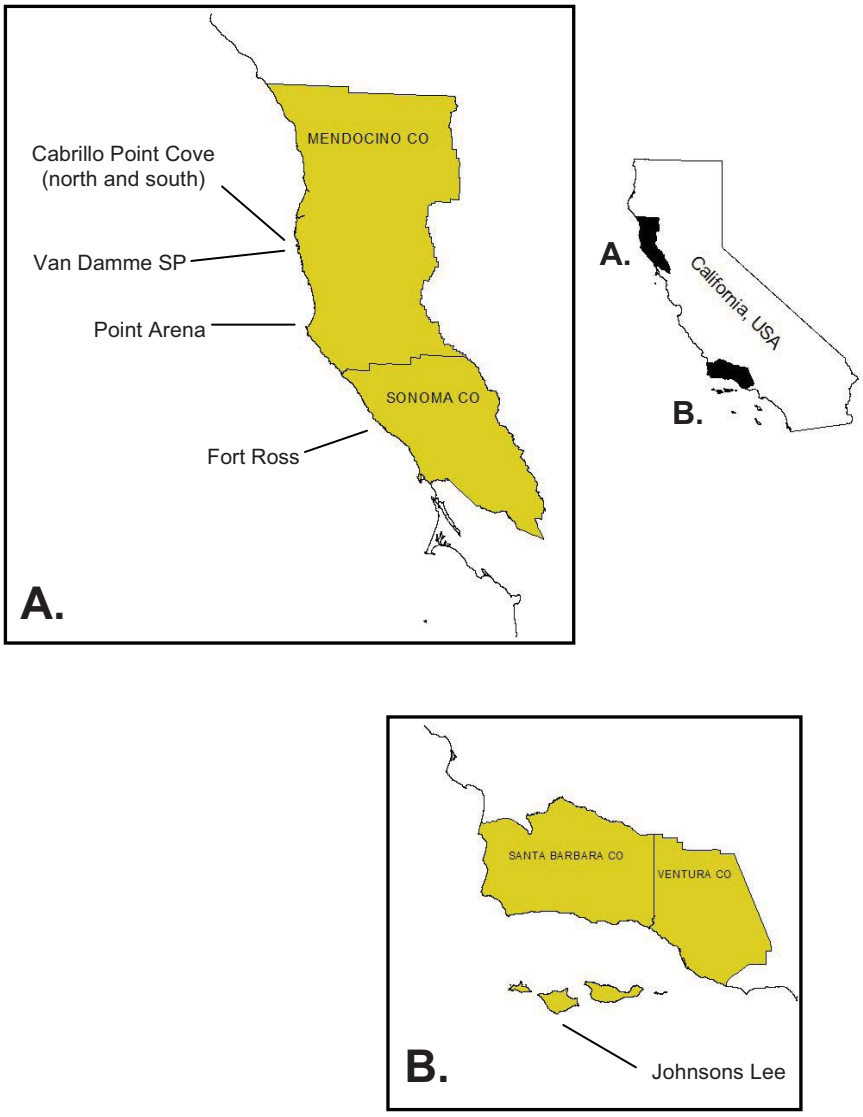

Figure 1. Map of northern (A) and southern (B) California study sites where tag-recapture work was performed. See text for geographic coordinates of each study site.

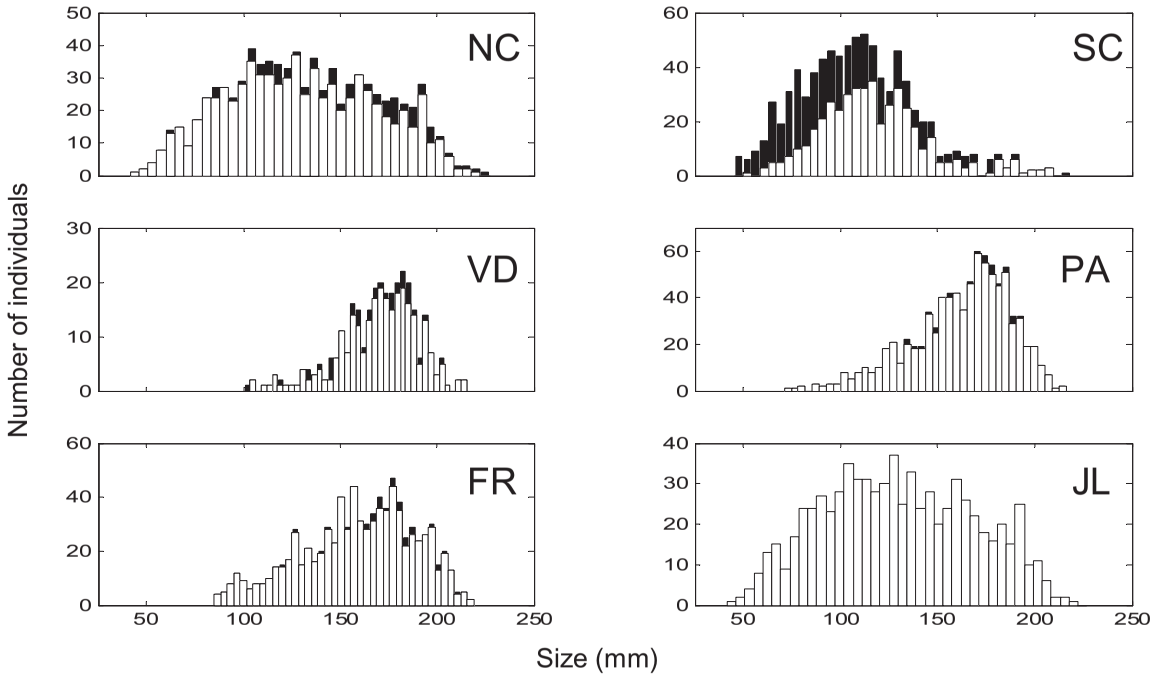

Figure 2. Size frequency distributions of tagged red abalone, retained (white) or removed (black), from analysis at each site in northern California (North Pt. Cabrillo Cove (NC), South Pt. Cabrillo Cove (SC), Van Damme State Park (VD), Pt. Arena (PA), and Fort Ross State Park (FR)) and southern California (Johnsons Lee (JL)).

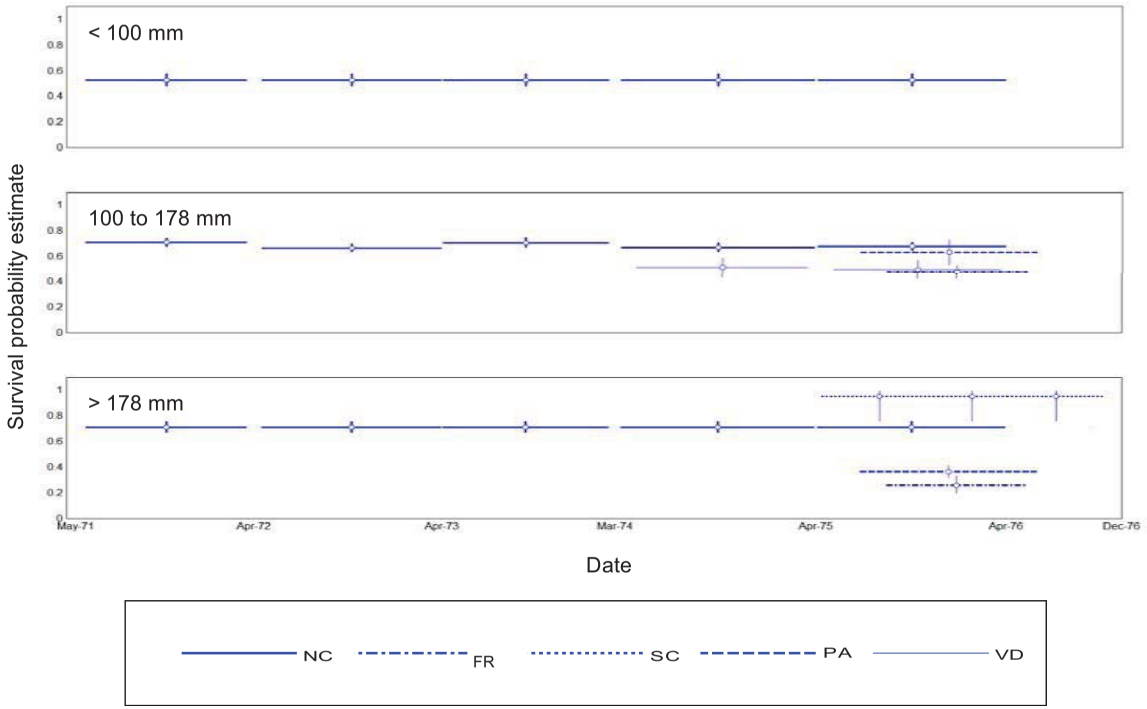

Figure 3a. Annual survival probability estimates from individuals in each size class (< 100 mm, 100 to 178 mm, and > 178 mm) from tag and recapture data from northern California sites North Pt. Cabrillo Cove (NC), South Pt. Cabrillo Cove (SC), Van Damme State Park (VD), Pt. Arena (PA), and Fort Ross State Park (FR) . ○ indicates median date of period for which tagged individuals were at large. Error bars are standard error (SE).

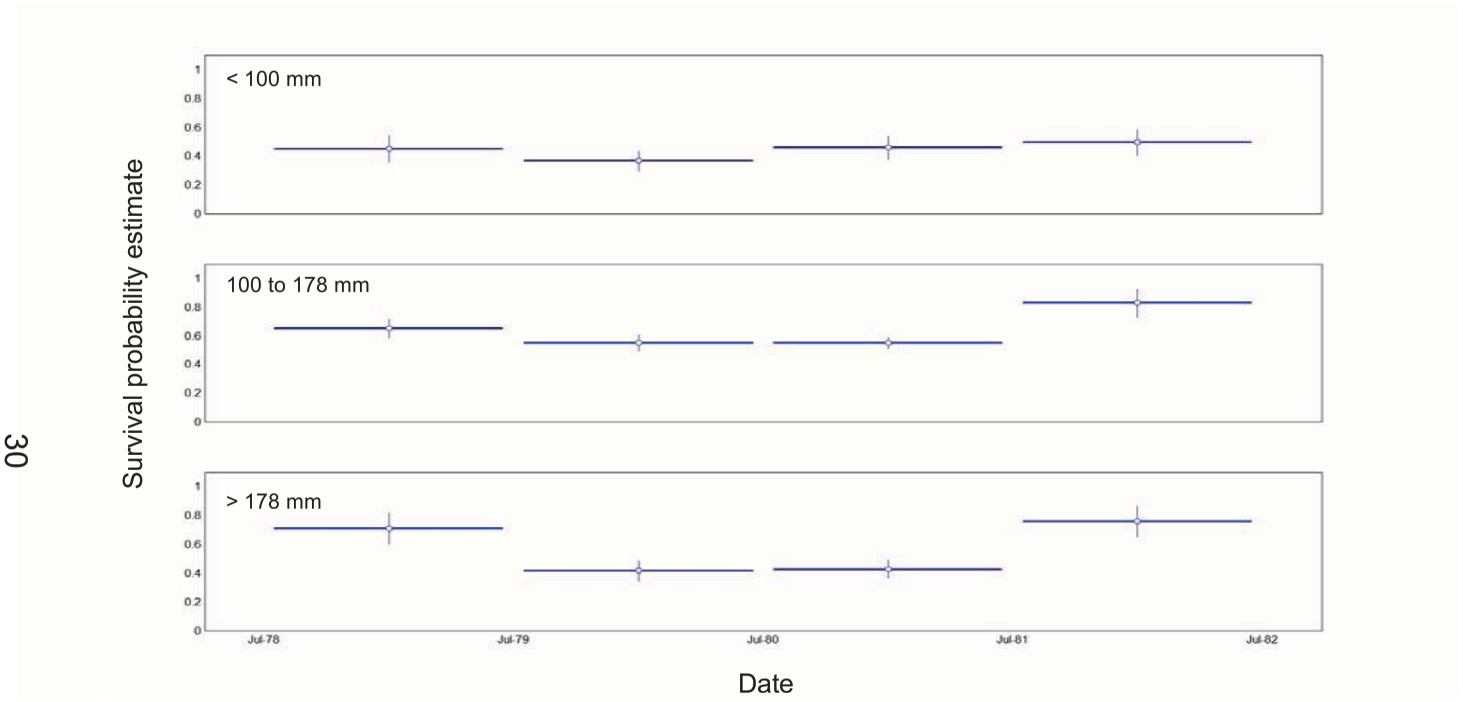

Figure 3b. Annual survival estimates from individuals in each size class (< 100 mm, 100 to 178 mm, and > 178 mm) from southern California tag and recapture data from site Johnsons Lee, JL. ○ indicates median date of period for which tagged individuals were at large. Error bars are standard error (SE).

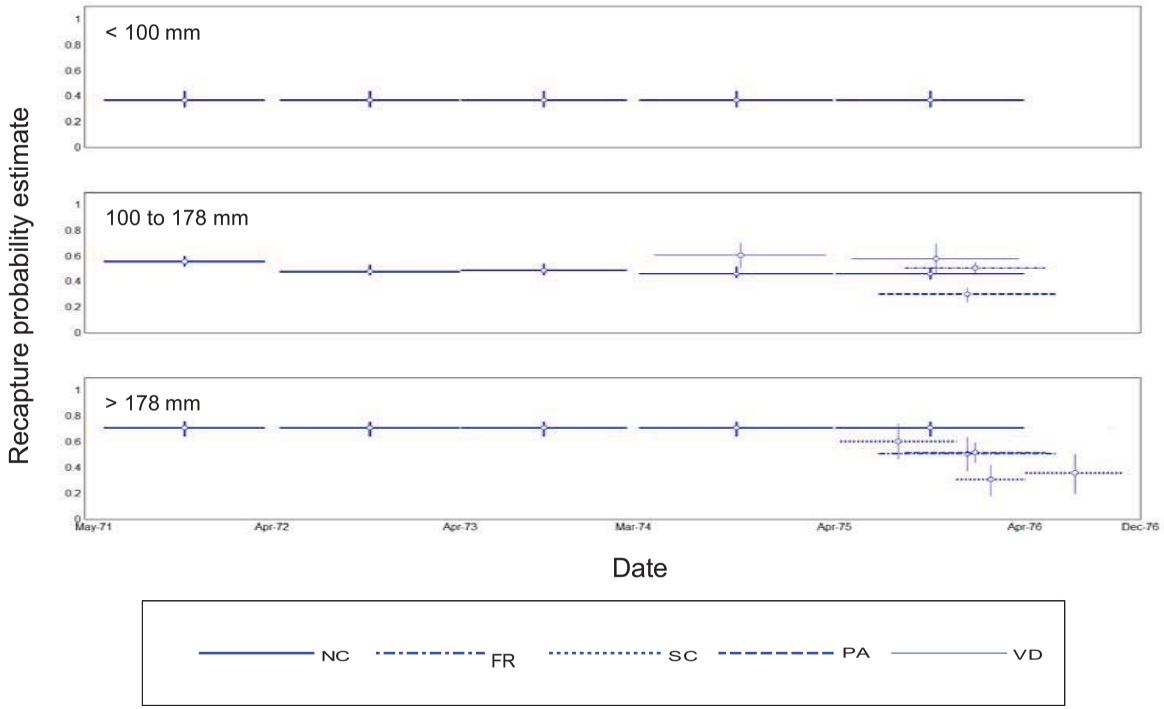

Figure 4a. Annual recapture probability estimates from individuals in each size class (< 100 mm, 100 to 178 mm, and > 178 mm) from tag and recapture data from northern California sites North Pt. Cabrillo Cove (NC), South Pt. Cabrillo Cove (SC), Van Damme State Park (VD), Pt. Arena (PA), and Fort Ross State Park (FR) . ○ indicates median date of period for which tagged individuals were at large. Error bars are standard error (SE).

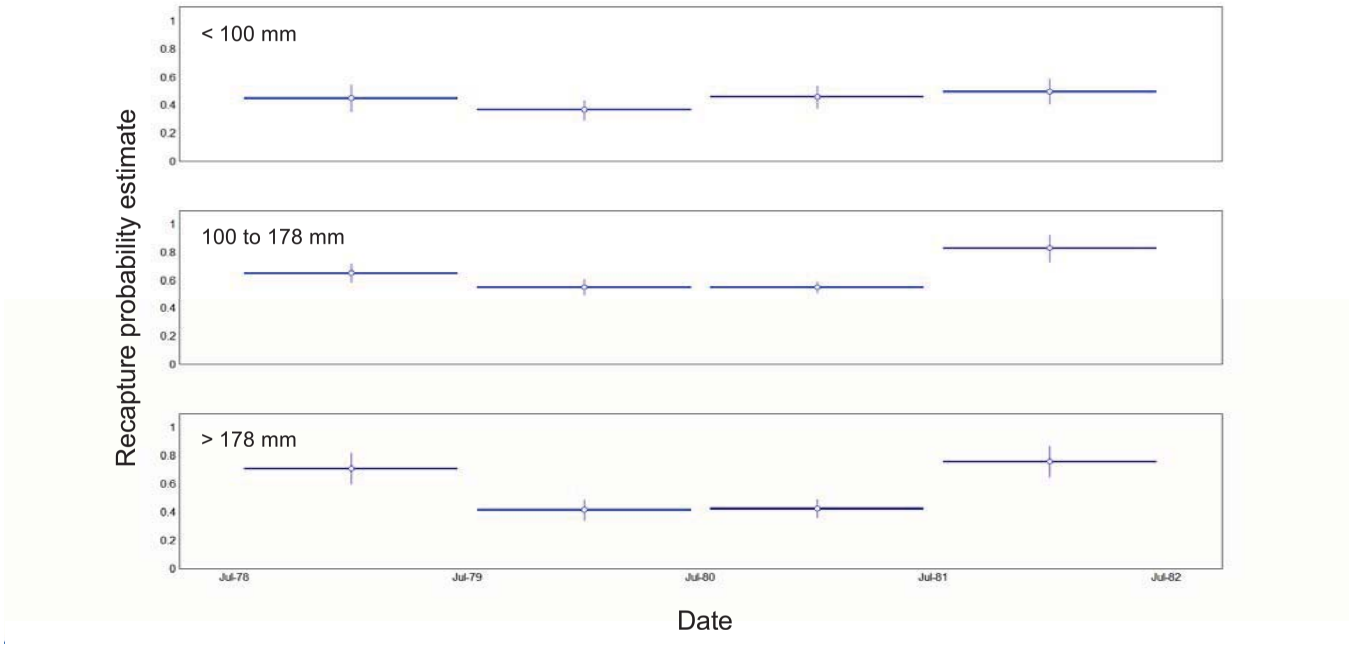

Figure 4b. Annual recapture estimates from individuals in each size class (< 100 mm, 100 to 178 mm, and > 178 mm) from southern California tag and recapture data from site JL. ○ indicates median date of period for which tagged individuals were at large. Error bars are standard error (SE).

CHAPTER 2

A size-based projection matrix model and elasticity analysis of red abalone, *Haliotis rufescens*, in northern California

ABSTRACT

Prospective elasticity analyses have been used to aid in the management of fished species. A size-based projection matrix model of red abalone, *Haliotis rufescens*, in northern California was constructed and elasticity values determined to evaluate the relative contribution of vital rates of each size class (n = 8) to the population growth rate (λ). Annual growth transitions (g_x) were determined from tagged and recaptured individuals (n = 560) from six locations. Fecundity, f_x, the number of viable eggs produced per female was determined from a four year reproduction study. Population growth rate (λ) was set to 1.0 and the first year survival (larval survival through to the first size class) was estimated by iteration. Elasticity values of survivorship and growth (summed p_x and g_x) and fecundity (f_x) were determined for each size class. Elasticity values were found to be greatest for the sub-legal red abalone 150 mm to 178 mm (MSL) indicating that changes in the vital rates of this size class are most important to λ. Alteration of size class divisions and vital rates did not result in changes to the relative ranking of elasticity values, suggesting that this model is robust to variations in model structure and vital rate data. These results suggest that the 178 mm (MSL) recreational size limit is set appropriately and that this size limit should not be decreased. This work is an example of how size-based projection matrix models can be used to evaluate the efficacy of fishery management and conservation strategies.

INTRODUCTION

Matrix population models are powerful demographic tools for addressing management and conservation issues (Crouse et al. 1987, Lande 1988, Heppell et al. 1994). Quantitative vital rate information can be incorporated into matrix models to explore the consequences of various management and conservation options (Caswell et al. 1998, Ebert 1999, Morris et al. 1999). Perturbations of these models, by simulation, allow comparison of vital rates and the determination of those most important to population growth (Benton and Grant 1999). This type of "forward looking" or prospective sensitivity analysis (Caswell 2000) has been used to evaluate management strategies and life history patterns for a variety of vertebrate and invertebrate taxa.

Perturbation analyses of loggerhead sea turtle matrix models lead to a redirection of conservation efforts away from "headstarting" hatchlings (enhancing the survival of eggs in nests) toward the use of turtle exclusion devices in fishing nets (reducing adult mortality) (Crouse et al. 1987, Crowder et al. 1994). In an analysis of a size-structured matrix model of red sea urchin, Ebert (1998) found that survivorship of the smallest sized individuals had the least effect on population growth rate and need not be the focus of management efforts. Long-lived, slow-growing species such as abalone may fit into a group of species that respond to perturbations in a stereotypical way with low fertility elasticities and high juvenile or adult survival elasticities (Heppell et al. 2000, Sæther and Bakke 2000, Gerber and Heppell 2004). For management and conservation of abalone it is important to recognize those size classes that that are most important to population growth rates.

Elasticity analysis, the proportional sensitivity of vital rates, can be used to evaluate decisions regarding the management of red abalone, *Haliotis rufescens* in California. The recreational red abalone fishery in northern California is now the only abalone fishery open in the state. Recreational and commercial abalone fisheries in southern California were closed in 1997 (California Senate Bill 463). Failure to manage individual species masked serial depletion of the species complex by the fishery (Dugan and Davis 1993, Karpov et al. 2000). In addition, predatory sea otters expanded their range in central California (Wendell 1994, Vogel 2000) while there may have been unfavorable environmental conditions for red abalone (Hobday and Tegner 2002). To date, there have been few quantitative evaluations of the efficacy of the current size limits and the other management strategies used in this fishery (but see Tegner et al. 1989). Assessments have been hindered by a lack of vital rate information for red abalone in northern California.

I used vital rate information for red abalone from archived California Department of Fish and Game data and published work to construct a deterministic size-structured matrix model (Lefkovitch 1965). Growth and survival estimates were derived from an extensive multi-year, multi-site tag-recapture study in northern California. Estimates of size-specific fecundities were derived from a 4-year reproduction study that quantified egg density (Rogers-Bennett et al. 2004). Because survival for the first year (from fertilized egg to age one) is unknown for abalone I assumed that population growth rate was stable (the dominant eigenvalue of the projection matrix, λ, was 1.0) and solved for first year survival, p_0, by iteration (Vaughan and Saila 1976). Elasticity values (Caswell 1978, de Kroon et al. 1986) were calculated to determine which size classes of red abalone had the

greatest influence on the intrinsic rate of population increase in the model and to determine if these size classes are being protected by the current fishery management regulations. Identification of these sensitive size classes and vital rates are valuable for the quantitative evaluation of research priorities, management policies and conservation strategies (Morris and Doak 2003).

METHODS

Red Abalone Mark and Recapture Field Study

Red abalone were tagged at five sites in northern California: North Pt. Cabrillo Cove (NC) and South Pt. Cabrillo Cove (SC) (39.364º N, 123.830º W), Van Damme State Park (VD) (39.274º N, 123.791º W), Pt. Arena (PA) (39.269º N, 123.799º W), and Fort Ross State Park (FR) (38.512º N, 123.244º W) (Figure 1). This tagging program was initiated in 1971 and recaptures were conducted at approximately annual frequencies. Red abalone were collected by divers, brought to the boat, maximum shell length (MSL) measured, and tagged with individually labeled stainless steel disc tags. Tags were attached with stainless wires inserted into the two open respiratory pores distal to the umbo and then twist tied. Red abalone tagged at the five sites ranged in size from 41.5 to 227 mm MSL (Table 1). Growth data from a total of 845 abalone recaptured at one year intervals plus or minus 30 days (335 to 395 days) was used in the analysis of growth transition rates. Growth was normalized for all individuals to one year by determining the daily growth rate and then standardizing to 365 days.

To supplement annual growth data for small (< 100 mm) individuals, data an additional tagging studies (Rogers-Bennett and Pearse 1998) were used. Growth information from this study were obtained from data from tagged juveniles out-planted at five sites in northern California in October 1995 and juveniles were recaptured one year later at Horseshoe Cove (38.316º N, 123.070º W). The size at the time of stocking from 5 to 29 mm (Table 1). The pale blue/green coloration allowed for the measurement of shell length at the time of stocking (initial) and the difference between the initial and the final shell length (blue plus red shell) gave a measure of growth during the year.

Growth Transition Matrix Construction

A growth transition matrix of the probability of an individual changing size classes annually was constructed from the observed changes in lengths of recaptured abalone. Columns are an individual abalone's first length measure and rows are their sizes one year later. The probability of transfer from one size class to another by an individual was determined by assigning each abalone into the column representing the initial size and the row representing the final size. This accounting for each is converted into a probability by dividing the number of individuals in each row (the number in each size class at t = 1) by the sum the individuals in each column (total number of individuals in the size class at t = 0). The results yield a matrix in which diagonal elements represent the probability of staying within a size class after 1 year and the elements in the sub-diagonal (below the diagonal elements) are the probability of growing into (transferring to) the larger size class.

Elements below this represent the probability of skipping a size class or growing into the next largest size class.

Size categories were selected to minimize both sampling and distribution error (Vandermeer 1978, Moloney 1986, Caswell 2001). Sampling errors arise when too few animals are sampled within a size class. Size class divisions were restricted such that no class contained fewer than 2 animals. Distribution errors arise because the model treats all animals within a size class equally, when in fact, some are at the start of the size class (left boundary) and some are closer to the end (right boundary) of the size class at the beginning of the year. To minimize distribution errors, size classes should be as narrow as allowed by sampling error.

I used the Moloney-Vandermeer algorithm (Vandermeer 1978, Moloney 1986, Caswell 2001) to contribute more information to the size class determinations in an effort to minimize both the sampling and the distribution errors. Sampling and distribution errors were minimized at very large size classes such that the matrix would have had six size classes (0.1 to 28 mm, 28.1 to 55 mm, 55.1 to 100 mm, 100.1 to 156 mm, 156.1 to 191 mm, and > 191 mm. These recommended size classes would not have allowed me to address the elasticity values for those size classes less than or greater than the current size limit, one objective of this study. Furthermore, the sampling and distribution errors reflect only one of the vital rates (growth) and did little to account for the two other vital rates (Caswell 2001).

The boundaries of the first size class were set such that they encompassed growth in the first year from 0.1 mm, the size at settlement, to the size at one year approximately 25

mm (Haaker et al. 1998, Rogers-Bennett et al. 2004). I set this as the size class interval, but deviated slightly at the larger sizes adjusting the size category from 175 to 178 mm to allow for a break at the minimum legal size for red abalone. The size at first reproduction is 105 mm (Rogers-Bennett et al. 2004) and is close to the boundary of the fourth size class of 100 mm. The structure of the growth data derived from the annual recaptures would not support smaller size class widths such as 20 mm since no animals remained in the second and third size classes and no animals remained or advanced in the largest size class. Comparable growth transition results were obtained with 29, 30, 31, and 35 mm size classes, matrices with these size class intervals resulted in no individuals transitioning to the largest size classes resulting in truncated size distributions when these matrices were numerically projected.

Annual Survival Probability Estimate

Survivorship was estimated using the tag-recapture profiles of 746 individually tagged red abalone censused at approximately annual intervals (339 to 398 days) at North Point Cabrillo Cove (39.364º N, 123.830º W), a no-fishing reserve, from March 1971 to April 1977. Annual tagging and recapture surveys were restricted to periods ranging from 2 to 38 days each year during March, April, and May. Tagged red abalone that were recovered between sampling periods were excluded from analysis because in many cases it was not possible to determine the fates of these individuals. Tag-recapture histories (n = 746) were converted to a vector format of tagged (ones) and untagged (zeros) following Lebreton et al. (1992).

Two groups of a posteriori models were specified to examine the archived tagging data. The first group consisted of two models in which the probability of survivorship (φ) was constant, denoted ($\varphi.$), and rates of recapture were time-dependent (p_t) and constant ($p.$) for all individuals in each size class. The second model group consisted of partitioning the data into three groups based on the size of individuals at the time of first tagging; individuals < 100 mm (n = 179), 100 to 178 mm (n = 470), and > 178 mm (n = 97). These size classes were determined based on the ecology and fishery biology of the species such that the classes represent respectively the "cryptic", "emergent sub-legal" and "emergent legal" size classes of the population. For each of the size classes a "global model" was defined ($\varphi_t p_t$) for which all estimates of survival and probability were fully time dependent. Each of the global models were tested for goodness-of-fit (GOF) with Program Release GOF tests 2 and 3 to determine whether the observed recapture histories conformed to Cormack (1964), Jolly (1965), and Seber (1965) assumptions; homogeneity of capture and survivorship (Burnham et al. 1987). Parametric re-sampling was used to assess global model dispersion, $\hat{c}$. If the global model deviance/mean of re-sampled model deviance was > 1, $\hat{c}$ was adjusted for all models with this new estimate.

Model groups with satisfactory global models were examined using the 'recaptures only' protocol in program MARK to determine annual survivorship and recapture rates by maximum likelihood estimation of the population (White and Burnham 1999). The quasi-likelihood criterion, QAIC, was used (Burnham and Anderson 1998) to rank candidate models. Mean annual survivorship and variances for equivalent candidate models were

computed using weighted averaging based on QAIC values of the two candidate models (Buckland et al. 1997).

Fecundity

Size-specific red abalone fecundity was determined from published work of Rogers-Bennett et al. (2004). Their work consisted of sampling gonad tissue from animals collected at Van Damme State Park (39.274º N, 123.791º W) and Point Arena (39.269º N, 123.799º W) in northern California. Abalone ranged in size from 29-224 mm maximum shell length (n = 107). Abalone were detached from the shell, weighed and dissected to estimate the gonad volume and obtain gonad tissue samples. Gonad volumes were estimated assuming that the gonad was cone shaped and wrapped around an inner cone of digestive gland. The volume of gonad was equal to the gonad/digestive gland complex minus the digestive gland cone (as per Tutschulte 1976).

To estimate the number of mature eggs in each female ovary, slide preparations were made and used to quantify egg number (see methods Rogers-Bennett et al. 2004). The number of eggs enumerated on each slide was then multiplied by the width of the tissue section and the ovary volume to obtain the number of eggs spawned in one year for each female. Fecundity was defined as the number of mature eggs present in the ovary (f_x). Mature oocytes averaged 170-190μm diameter, were circular in shape and detached from the trabeculae ready to be spawned.

The relationship between female size and mature egg number was modeled using a three parameter Gaussian curve (Figure 2). This curve was used to estimate the number of

mature eggs produced per year by in each size class. The relationship between shell length (X) and egg number (Y) was modeled by the curve in the form:

$$(Y) = Ae^{-(X-\mu)^2/2\sigma^2}$$

A = 2,850,000 eggs per female (SE = 1,079,000 eggs)
μ = 215 mm,
σ = 38 mm,

A is defined as the maximum productivity, μ is defined as the size at maximum productivity, and σ the standard deviation describes the width of the distribution of maximum productivity *vs*. size.

Size-Based Red Abalone Matrix

A size-structured matrix model with 9 size classes, of 25 mm, was constructed for red abalone, assuming a pre-breeding, birth-pulse population. First, growth transition rates were determined using tag recapture data of abalone growing for one year (Table 4). In some cases the data suggest some backward growth transitions for 6 and 12% of the two largest size classes, respectively. Growth transition probabilities were then multiplied by annual survivorship. Second, egg number for each size class was the mean fecundity for the median sized females for each size category using the Gaussian curve estimates. The number of mature eggs was then divided by two to be the number of female offspring produced by a female in a year (f_x) (assuming a 50/50 sex ratio). Third, the first row and column of the size transition matrix representing growth and survival, p_0, of individuals 0.1 to size 25mm are subsequently dropped from the matrix. And fourth, in the pre-breeding

census, (f_x) is multiplied by p_0, which is equal to the fertilization success, survival in the larval stage and post settlement stages in the first year. Then, p_0 was solved by iteration by assuming that the population growth rate λ, is 1.0 (with a population growth rate, λ = 1.0039), and is stable (Vaughan and Saila, 1976). First year survivorship, after iteration was $p_0 = 1.53 \times 10^{-6}$, and was incorporated into f_x values to construct the population projection matrix (Table 5).

Elasticity, Stable size distribution (SSD) and parameter uncertainty

The elasticity values of fecundity, which incorporated first year survival ($f_x * p_0$), and growth and survival were determined for each size class. Elasticity of a matrix element, e_{ij}, is the sensitivity value scaled to incorporate the magnitude of both λ and the matrix element. Elasticity is frequently used instead of sensitivity because reproduction and growth transitions measures are measured on different scales and $\Sigma e_{ij} = 1.0$ (de Kroon et al. 1986). Elasticity values of matrix elements were calculated using PopTools (G. Hood, CSIRO http://www.dwe.csiro.au/vbc/poptools/).

$$e_{ij} = \frac{a_{ij}}{\lambda} \frac{\partial \lambda}{\partial a_{ij}}$$

To examine how variation in the mean values of the parameters of fecundity and survival contribute to uncertainty in elasticity values a number of matrix simulations were performed. Elasticity values were determined from matrices that were constructed using the minimum and maximum values of the fecundity and survival estimates (Mills et al.

1999, Hunter et al. 2000). Minimum annual survival was calculated as the mean of the estimated survivorship for each size class minus one standard error. Maximum annual survival was calculated as the mean of the estimated annual survivorship plus one standard error. The minimum and maximum fecundity estimates were calculated as the minimum or maximum number of eggs produced for and individual in each size class.

To determine how variations in the width of the size classes of the growth transition matrix with 25 mm increments may contribute to errors in the elasticity values of size classes of the matrix projection model, I constructed a pre-breeding, post census model based on the size classes recommended by the Moloney-Vandermeer algorithm. Fecundity for each size class was determined using the Gaussian regression estimate of the median sized individual for each size class. Elasticity values for fecundity and growth and survivorship were calculated for each size class. To allow comparisons between the two size-structured models, the 25 mm and the Moloney-Vandermeer specified model, I used an annual survivorship rate of $\varphi = 0.684$ for all size classes for both models.

RESULTS

Annual survivorship estimates

The fit of the global survival model for recapture histories of all sizes of red abalone as a group was poor based on binomial dispersion ($\hat{c}$) and Release GOF tests (Table 2). Model fit was improved by partitioning the recapture data into the three size classes. Binomial dispersion, $\hat{c}$, of the global model was reduced for each of the partitioned

size classes in comparison to the grouped recapture histories. The > 178 mm size class had reduced $\hat{c}$ values and non-significant GOF Tests 2 and 3. It was not possible to test data for the size class < 100 mm for GOF Test 3 due to low sample sizes, however Test 2 fit the data satisfactorily. Size class 100 to 178 mm passed Test 2 ($p = 0.0783$), however it failed Test 3 ($p = 0.0011$).

For those individuals less than 100 mm and > 178 mm the model with constant survivorship ($\varphi.$) and recapture ($p.$) was favored over competing models. There was little difference between the two models ($\varphi.p.$) and ($\varphi.p_t$) for the 100 to 178 mm size class (ΔQAIC $<$ 2.0). For abalone less than 100 mm survival was estimated as $\varphi = 0.526$ ($\pm$0.051 SE), survival of 100 to 178 mm abalone was estimated as $\varphi = 0.684$ ($\pm$0.024 SE), and survivorship of abalone > 178 mm was $\varphi = 0.709$ ($\pm$0.046 SE).

Red Abalone Matrix Construction: SSD, Elasticity, and Simulations

The stable size distribution predicted by the red abalone matrix was dominated by small size classes and the proportion of individuals decrease with increasing size (Figure 3A). The relatively low survivorship predicted for each size class resulted in the projected population to have very few individuals in largest size classes.

The larger sizes had the most reproductive value with individuals in the > 200 mm size class having the most reproductive value (35%) based on the projected values of reproduction (Figure 3B). The mean levels of reproduction per size class are greatly increased for the larger size classes, after individuals reach 150 mm.

The proportional elasticity of the red abalone matrix suggests that the matrix element composed of vital rates of remaining in and surviving in the 7th size class (150-178 mm) had the largest summed elasticity (0.247) and therefore the most influence on population growth rate λ of the model (Figure 3C). Survival and growth made up 88% of the elasticity value while reproduction comprised 12%. Elasticities for survival (p_x) were much greater than for reproduction (f_x) for each size class. Eliminating the backward growth transitions did not alter the relative ranking of size class elasticities and their influence on λ.

The relative rankings of the elasticity values of each size class is robust to changes in vital rates over the range of minimum and maximum fecundity and annual survivorship values examined in comparison to the mean vital rates (Figure 4). Simulations suggest that changing fecundity values had minimal impact on elasticity values in the model as compared with changing survival values from the mean to their minimum and maximum values. Minimizing variability in survival estimates would improve model prediction more than minimizing variability for fecundity.

Although the relative elasticity values for each size class changed when size class divisions were altered from the 25 mm to the Moloney-Vandermeer divisions, there was a correspondence of the general size-specific elasticity patterns (Figure 5). The largest size classes for both matrices had the smallest summed elasticity values of each size class. The median size classes for the Moloney-Vandermeer matrix (100.1 to 191 mm, n = 2) and the 25 mm division matrix (100.1 to 200 mm, n = 4) had greater summed elasticity values than

the preceding size classes. The 55.1 to 100 mm (n = 1, 25 mm divisions) and 50.1 to 100 mm (n = 2, Moloney-Vandermeer divisions) had similarly low relative values.

DISCUSSION

Elasticity values of red abalone in northern California were determined using a size-based Lefkovitch matrix population model. Lefkovitch models have been used to explore the population dynamics of organisms whose vital rates co-vary with size or stage (Ebert 1999). Lefkovitch models are also useful for organisms that are difficult to age such as marine algae (Åberg 1990, 1992a,b, Ang and De Wreede 1993), urchins (Ebert 1998), and gorgonians (Gotelli 1991). Mollet and Cailliet (2002) have documented that some population dynamics, including reproductive rate and generation time, as estimated by Lefkovitch models differ in comparison to those predicted by Leslie matrices and life-history tables. Additionally, they noted that Lefkovitch models predict shorter recovery times to the stable stage distribution, after perturbation, in comparison to age based methods.

The differences in the observed dynamics of Lefkovitch models to their age-based equivalents are a result of arbitrary selection, by the experimenter, of the widths of size classes. The Moloney-Vandermeer algorithm (Vandermeer 1978, Moloney 1986, Caswell 2001) aids experimenters in reducing the error inherent in the structure of available growth transition data. However, the Moloney-Vandermeer algorithm does not address how changing the stage/size interval and by extension altering the number of resulting stage/size

classes influences the results of model projection. Examination of Lefkovitch models of plant and elasmobranch populations, in which the designation of a few wide size classes increase the probability of retention of individuals, results in greater elasticity values for those classes (Enright et al. 1995, Mollet and Cailliet 2002). To remedy the potentially spurious results of Lefkovitch matrices, Crouse et al. (1987) have incorporated intra-stage probability distributions to more realistically model individual growth and survivorship. In this study I have included enough size classes such that the minimum time for an individual starting in the first stage to graduate to the minimum size to fishery (> 178 mm) is seven years, which is biologically reasonable (Haaker et al. 1998).

Easterling (1998) and Easterling et al. (2000) presented a size-structured model that eliminates the error in elasticity values associated with the arbitrary division of a population into size classes. This model, called the 'integral projection model', treats growth, fecundity, and survivorship of individuals as a continuous function of an individual's size. The integral projection model has been shown to be robust in comparison to traditional matrix projection methods and has been used to describe the dynamics of plant populations whose vital rates are size-related (Easterling 1998, Easterling et al. 2000, Rees and Rose et al. 2002, Childs et al. 2003). This model is a promising method to explore for red abalone population dynamics. However, it will be necessary to describe annual survivorship as a continuous function of size for this method to be used.

Elasticity values of the projection matrix in this study are derived from mean values of vital rates (annual survivorship, fecundity, and growth) incorporated into a deterministic (time-invariant) matrix model. While little is known about temporal variability of vital rates

in abalone populations (Shepherd and Breen 1992), the assumption that they are static is unlikely (Benton and Grant 1996). I estimated annual survivorship from two models using the Cormack-Jolly-Seber model (Cormack 1964, Jolly 1965, Seber 1965). In both models the survivorship component was constrained to be constant ($\varphi.$). The fit of the time invariant models ($\varphi. p.$ and $\varphi. p_t$) for each of the three size classes was favored over time varying survivorship for the < 100 mm and > 178 mm size classes. The time invariant models ($\varphi.p.$ and $\varphi.p_t$) had an equivalent fit to the time varying model ($\varphi_t p.$). These model selection results indicate that over the course of the tag and recapture study at North Point Cabrillo Cove the recapture history data support models in which survivorship is constant in time.

Rogers-Bennett et al. (2004) described size specific fecundity of red abalone and documented the variability in the relationship of size to egg production (Figure 2). However, they did not describe temporal variability in egg production. Dr. David Ebert (MLML, personal communication) reported that in 1966-67 and 1995-96 few reproductively active female red abalone throughout California could be found. The majority of the red abalone in California had inactive gonads, indicating that in some years there is poor egg production for these populations. Haaker et al. (1998) documented significant changes in growth of red abalone that resulted in a range of time to attain 178 mm (MSL) from seven to 25 years. Pooled growth transition data from multiple years and six sites does not allow description of the heterogeneity of this vital rate. However, a Monte-Carlo approach could be used to generate growth transition matrices from available data or from the observed variances of the Von Bertalanffy growth function to generate

growth transitions. To address the robustness of the matrix model to variations in vital rates, as might be expected in a stochastic environment, I used the high (mean + 1 SD), mean, and low (mean – 1 SD) values of reproduction and survival estimates (Mills et al. 1998). These simulations did not affect the ranking of the elasticity values suggesting that the static model is robust to stochastic changes in vital rates over the range of values examined (Figure 3A).

Elasticity results in this study suggest that the current minimum legal size (178 mm) in the recreational red abalone fishery is set appropriately; protecting the size class that most influences population growth in the model. In a similar analysis of red sea urchins (Ebert 1998) the largest size classes had the most influence on population growth rates. In this case the commercial sea urchin fishery may benefit from an upper limit, in addition to the existing lower size limit (Ebert 1998). Adult survival in other long-lived marine organisms such as loggerhead sea turtles (Crouse et al. 1987) and gorgonians (Gotelli 1991) had the most influence on population growth supporting the hypothesis of a relationship between life history strategy and elasticity values (Heppell et al. 2000, Cortes 2002).

The elasticity results of the red abalone model suggest that enhancement in survival of sub-legal red abalone in the model would have the greatest impact on population growth. Enforcement efforts, education, and research in this area could benefit the fishery. Abalone have no blood clotting mechanism and will bleed to death if they are cut during fishing with abalone irons. Research could be directed at uncovering the causes of mortality including incidental mortality of sub-legal animals associated with fishing. Marine

protected areas may be another tool which could benefit red abalone by reducing incidental mortality of the critical size class from incidental mortality (Gerber and Heppell 2004).

LITERATURE CITED

Åberg, P. 1990. Measuring size and choosing category size for a transition matrix study of the seaweed *Ascophyllum nodosum*. Marine Ecology Progress Series 63: 281-287.

Åberg, P. 1992a. A Demographic study of two populations of the seaweed *Ascophyllum nodosum*. Ecology 73(4): 1473-1487.

Åberg, P. 1992b. Size based demography of the seaweed *Ascophyllum nodosum*, in stochastic environments. Ecology 73(4): 1488-1501.

Ang, P.O., Jr. and R.E. De Wreede. 1993. Simulation and analysis of the dynamics of a *Fucus distichus* (Phaeophyceae, Fucales) population. Marine Ecology Progress Series 93: 253-265.

Benton, T. G. and A. Grant 1999. Elasticity analysis as an important tool in evolutionary and population ecology. TREE 14:467-471.

Benton, T.G., and A. Grant 1996. How to keep fit in the real world: elasticity analyses and selection pressures on life-histories in a variable environment. American Naturalist 147:115-139.

Buckland, S.T., K.P. Burnham, and N.H. Augustin. 1997. Model selection: an integral part of inference. Biometrics 53: 603-618.

Burnham, K. P., and G. C. Anderson 1998. Model Selection and Multi-Model Inference: a practical information-theoretic approach, 2nd edition. Springer, New York.

Burnham, K. P., D. R. Anderson, G. C. White, C. Brownie, and K. H. Pollock. 1987. Design and analysis methods for fish survival experiments based on release-recapture. American Fisheries Society Monograph 5. 1-437.

Caswell, H. 2000. Prospective and retrospective perturbation analysis: Their roles in conservation biology. Ecology 81:619-627.

Caswell, H. 2001. Matrix Population Models: Construction, Analysis, and Interpretation. Sinauer Associates; 2nd edition. 722 pages

Caswell, H., Brault, S., Read, A. J., and T. D. Smith. 1998. Harbor porpoise and fisheries: An uncertainty analysis of incidental mortality. Ecological Applications 8:1226-1238.

Caswell, H. 1978. A general formula for the sensitivity of population growth rate to changes in life history parameters. Theoretical Population Biology 14:215-230.

Childs, D.Z., Rees, M., Rose, K.E., Grubb, P.J., and S.P. Ellner. 2003. Evolution of complex flowering strategies: an age- and size-structured integral projection model. Proceedings of the Royal Society of London B 270: 1829-1838.

Cormack, R.M. 1964. estimates of survival from the sighting of marked individuals. Biometrika 51:429-438.

Cortes, E. 2002. Incorporating uncertainty into demographic modeling: Application to shark populations and their conservation. Conservation Biology 16:1048-1062.

Crouse, D. T., Crowder, L. B., and H. Caswell 1987. A stage-based population model for loggerhead sea turtles and implications for conservation. Ecology 68:1412-1423.

Crowder, L. B., Crouse, D. T., Heppell, S. S., and T. H. Martin 1994. Predicting the impact of turtle excluder devices on loggerhead sea turtle populations. Ecological Applications 4:437-445.

de Kroon, H., Plaiser, A., van Groenendael, J. and H. Caswell 1986. Elasticity: The relative contribution of demographic parameters to population growth rate. Ecology 67:1427-1431.

Dugan, J. E. and G. E. Davis. 1993. Applications of marine refugia to coastal fisheries management. Canadian Journal of Fisheries and Aquatic Sciences 50:2029-2042.

Easterling, M.R. 1998. The integral projection model: Theory, analysis, and application. University of North Carolina, Raleigh, PhD dissertation.

Easterling, M.R., Ellner, S.P. and P.M. Dixon. 2000. Size-specific sensitivity: Applying a new structured population model. Ecology 81(3): 694-708.

Ebert, T. A. 1999. Plant and Animal Populations: Methods in Demography. Academic Press, San Diego.

Ebert, T. A. 1998. An analysis of the importance of Allee effects in management of the red sea urchin *Stongylocentrotus franciscanus*. Pages 619-627 *in* T. Mooi, editor. Echinoderms: San Francisco. Balkema, Rotterdam.

Enright, N.J., Franco, F. and J. Silvertown 1995. Comparing plant life histories using elasticity analysis: the importnace of life span and the number of life-cycle stages. Oecologia 104:79-84.

Gerber, L. R. and S. S. Heppell 2004. The use of demographic sensitivity analysis in marine species conservation planning. Biological Conservation 120:121-128.

Gotelli, N. J. 1991. Demographic models for Leptogorgia virgulata, a shallow-water Gorgonian. Ecology 72:457-467.

Haaker, P. L., Parker, D.O., Barsky, K.C., and C. S. Chun 1998. Growth of the red abalone, Haliotis rufescens (Swainson), at Johnsons Lee, Santa Rosa Island, California. Journal of Shellfish Research 17:747-753.

Heppell, S. S., Walters JR. and L. B. Crowder 1994. Evaluating management alternatives for red-cockaded woodpeckers - A modeling approach. Journal of Wildlife Management 58:479-487.

Heppell, S. S., H. Caswell and L. B. Crowder 2000. Life histories and elasticity patterns: perturbation analysis for species with minimal demographic data. Ecology 81:654-665.

Hobday, A. J., and M. J. Tegner 2002. The warm and the cold: Influence of temperature and fishing on local population dynamics of red abalone. CalCOFI 43:74-96.

Hunter, C. M., Moller, H., and Fletcher, D. 2000. Parameter uncertainty and elasticity analyses of a population model: Setting research priorities for shearwaters. Ecological Modelling 134:299-323.

Jolly, G.M. 1965. Explicit estimates from capture-recapture data with both dead and immigration-stochastic model. Biometrika 52: 225-247.

Karpov, K. A., Haaker, P. L., Taniguchi, I. K., and Rogers-Bennett, L. 2000. Serial depletion and the collapse of the California abalone (*Haliotis* spp.) fishery. Canadian Journal of Fisheries and Aquatic Sciences 130:11-24.

Lande, R. 1988. Demographic models of the northern spotted owl (*Strix occidentalis caurina*). Oecologia 75:601-607.

Lebreton, J. D., K.P. Burnham, J. Colbert, and D.R. Anderson 1992. Modeling survival and testing biological hypotheses using marked animals: A unified approach with case studies. Ecological Monographs 62:67-118.

Lefkovitch, L. P. 1965. The study of population growth in organisms grouped by stages. Biometrics 21:1-18.

Mills, L. S., D. F. Doak, and M. J. Wisdom 1999. The reliability of conservation actions based on elasticity analysis of matrix models. Conservation Biology 13:815-829.

Mollet, H.F. and G.M. Cailliet. 2002. Comparative population demography of elasmobranchs using life history tables, Leslie matrices and stage-based matrix models. Marine and Freshwater Research 53: 503-516

Morris, W. F. and D. F. Doak. 2003. Quantitative Conservation Biology: Theory and Practice of Population Viability Analysis. Sinauer Associates. Sunderland, Massachusetts.

Morris, W. F., D.F. Doak, M.Groom, P. Kareiva, J. Fieberg, L. Gerber, P. Murphy, and D. Thomson 1999. A Practical Handbook for Population Viability Analysis, The Nature Conservancy, Washington D.C.

Moloney,K.A. 1986. A generalized algorithm for determining category size. Oecologia 69:176-180.

Rees, M. and K.E. Rose. 2002. Evolution of flowering strategies in *Oenothera glazioviana*: an integral projection model approach. Proceedings of the Royal Society of London B 269: 1509-1515.

Rogers-Bennett, L., Dondanville, R.F. and J. V. Kashiwada. 2004. Size specific fecundity of red abalone (*Haliotis rufescens*): Evidence for reproductive senescence? Journal of Shellfish Research 23:553-560.

Rogers-Bennett, L. and J.S. Pearse. 1998. Experimental seeding of hatchery-reared juvenile red abalone *Haliotis rufescens* in northern California. Journal of Shellfish Research 17:877-880.

Sæther, B.-E. and O. Bakke 2000. Avian life history variation and contribution of demographic traits to the population growth rate. Ecology 81:642-653.

Seber, G.A.F. 1965. A note on the multiple-recapture census. Biometrika 52:249-259.

Shepherd, S.A. and P.A. Breen 1992. Mortality in abalone: its estimation, variability and causes. Abalones of the World: Biology, Fisheries and Culture. Fishing News Books, Victoria Australia.

Tegner, M. J., Breen, P.A., and Lennert, C.E. 1989. Population biology of red abalones, *Haliotis rufescens*, in Southern California and management of the red and pink, *H. corrugata*, abalone fisheries. Fishery Bulletin 87:313-339.

Tutschulte, T.C. 1976. The comparative ecology of three sympatric abalones. Dissertation U.C. San Diego, CA.

Vandermeer, J. 1978. Choosing category size in a stage projection matrix. Oecologia 32:79-84.

Vaughan, D. S., Saila, S.B. 1976. A method for determining mortality rates using the Leslie matrix. Transactions of the American Fisheries Society 3:380-383.

Vogel G. 2000. Migrating otters push law to the limit. Science 289:1271.

Wendell, F. E. 1994. Relationship between sea otter range expansion and red abalone abundance and size distribution in central California. California Department of Fish and Game Bulletin 80:45–56.

White, G.C. and K. P. Burnham. 1999. Program MARK: Survival estimation from populations of marked animals. Bird Study 46 Supplement, 120-138.

Table 1. Summary of capture mark recapture (CMR) statistics at sites from northern California from Schultz and DeMartini and Rogers-Bennett and Pearse (2004).

Site	# tagged	# recaptured one year after initial tagging	Number of years sampled	Size range at first tagging (mm)
Pt. Arena	1227	252	3	71 - 218
North Cabrillo Cove	837	137	7	41.5 - 227
South Cabrillo Cove	1774	58	3	41.5 - 223.5
Pedotti Ranch (Fort Ross)	1415	306	3	49.5 - 185
Van Damme	704	92	3	48 - 218.5
Juvenile out-plants Horseshoe Cove	NA	42	1	5 - 28.5
Total	5957	887		

Table 2. Goodness-of-fit test and model deviance of capture-mark-recapture histories from north Cabrillo Point (n = 746). Results derived from Program Release GOF (Burnham et al. 1987). *c_hat* values are the mean deviance of parametric resamples divided by the global model, $\bullet\ {}_{t}p_{t}$, deviance.

Size class (mm)	Test2			Test3			Test2 + Test3			
	X^2	df	p	X^2	df	p	X^2	df	p	*c_hat*
All	20.203	8	0.0096	41.6221	9	< 0.00001	61.825	17	< 0.00001	1.5112
< 100	3.4049	4	0.4925	-	-	-	-	-	-	1.0501
100 to 178	14.1363	8	0.0783	25.9294	8	0.0011	40.0656	16	0.0008	1.1721
≥ 178	1.9684	4	0.7416	4.2333	7	0.7525	6.2017	11	0.8596	1.0438

Table 3. Summary of information for model selection of competing models from capture-mark-recapture histories from north Cabrillo Cove. Estimates of the mean and variance of survival from models with equivalent model fits (QAICc < 2) (Burnham and Anderson 1998) were derived using their model AICc values as a weighting factor.

Size class (mm)	Number of individuals	Model	Number of parameters	AICc	Delta AICc	AICc weight	Model likelihood
All	746	$\bullet\ .\ p_t$	7	1332.42	0	0.44	1.00
		$\bullet\ .\ p.$	2	1334.50	2.08	0.16	0.35
< 100	179	$\bullet\ .\ p.$	2	355.55	0	0.72	1.00
		$\bullet\ .\ p_t$	7	357.76	2.2	0.24	0.33
100 to 178	470	$\bullet\ .\ p.$	2	1131.51	0	0.40	1.00
		$\bullet\ .\ p_t$	7	1131.57	0.06	0.39	0.97
> 178	97	$\bullet\ .\ p.$	2	261.13	0	0.91	1.00
		$\bullet\ .\ p_t$	7	267.96	6.83	0.03	0.03

Table 4. Annual growth transition probabilities of marked individuals. Columns are the length of an individual abalone at first census and rows are their sizes one year later. For example an individual starting in the 25.1 to 50 mm size class has a 50% probability of remaining in the size class and a 50% probability of tranistioning to the next size class, 50.1 to 75 mm, after one year.

Size class (mm)	0.1 to 25	25.1 to 50	50.1 to 75	75.1 to 100	100.1 to 125	125.1 to 150	150.1 to 178	178.1 to 200	> 200.1
0.1 to 25	0.600	0	0	0	0	0	0	0	0
25.1 to 50	0.375	0.500	0	0	0	0	0	0	0
50.1 to 75	0.025	0.500	0.100	0	0	0	0	0	0
75.1 to 100	0	0	0.800	0.281	0	0	0	0	0
100.1 to 125	0	0	0.100	0.649	0.301	0	0	0	0
125.1 to 150	0	0	0	0.070	0.677	0.483	0	0	0
150.1 to 178	0	0	0	0	0.022	0.517	0.917	0.062	0
178.1 to 200	0	0	0	0	0	0	0.083	0.926	0.120
> 200.1	0	0	0	0	0	0	0	0.012	0.880

Table 5. Size structured transition matrix of red abalone for northern California based on mean survival (p_x), growth transitions (gx), and fecundity (fx). Cells in the first row in columns with size classes $\geq$ 100.1 mm represent (g_x x p_0). Cells in the diagonal and sub diagonal are gx multiplied by size specific survivorship.

Size class (mm)	25.1 to 50	50.1 to 75	75.1 to 100	100.1 to 125	125.1 to 150	150.1 to 178	178.1 to 200	> 200.1
25.1 to 50	0.263	0	0	0.57	2.72	8.86	17.25	21.61
50.1 to 75	0.263	0.053	0	0	0	0	0	0
75.1 to 100	0	0.421	0.148	0	0	0	0	0
100.1 to 125	0	0.053	0.341	0.206	0	0	0	0
125.1 to 150	0	0	0.037	0.463	0.330	0	0	0
150.1 to 178	0	0	0	0.015	0.354	0.627	0.043	0
178.1 to 200	0	0	0	0	0	0.057	0.640	0.083
> 200.1	0	0	0	0	0	0	0.009	0.608

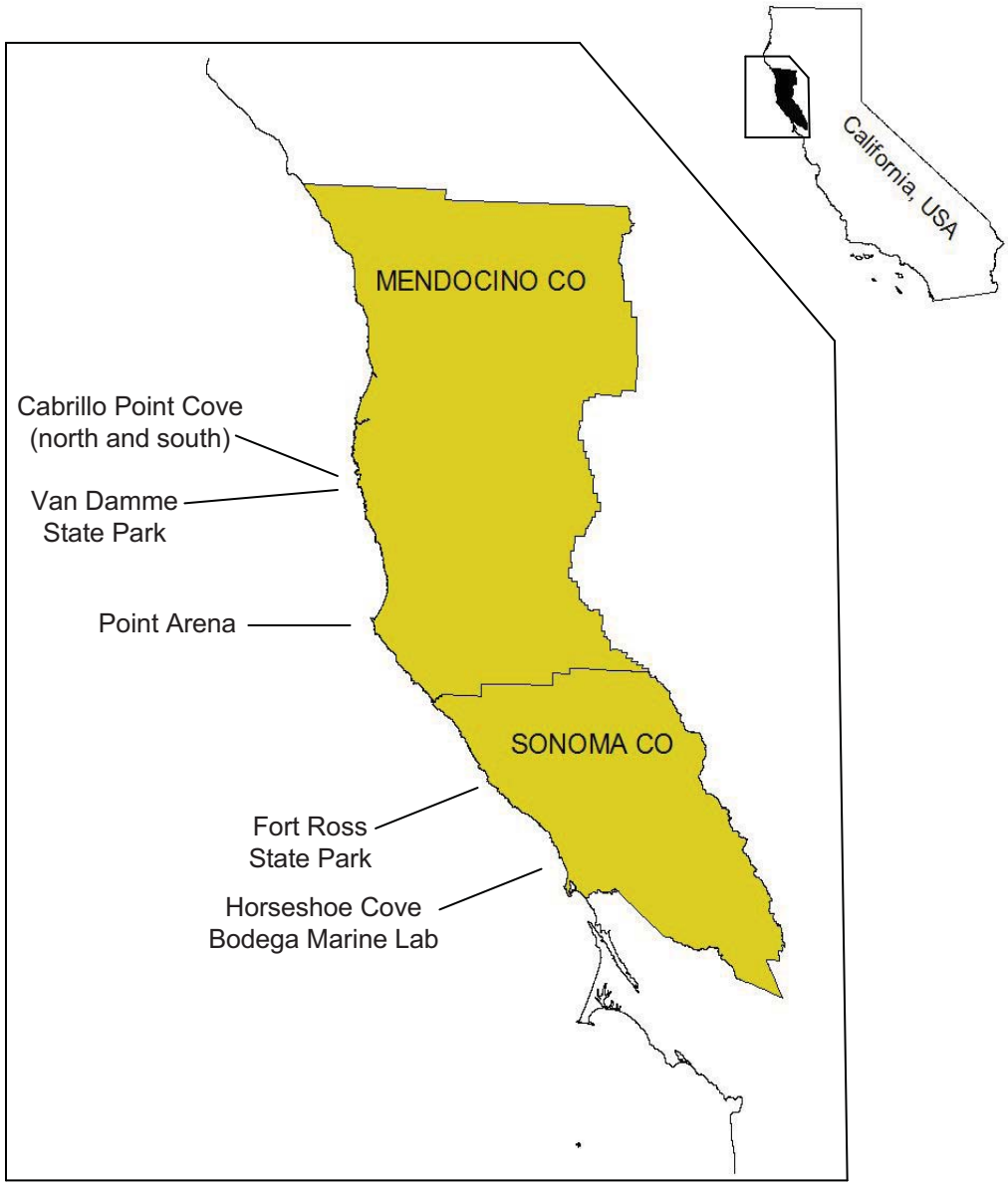

Figure 1. Map of northern California study sites where tag-recapture work was performed. See text for geographic coordinates of each study site.

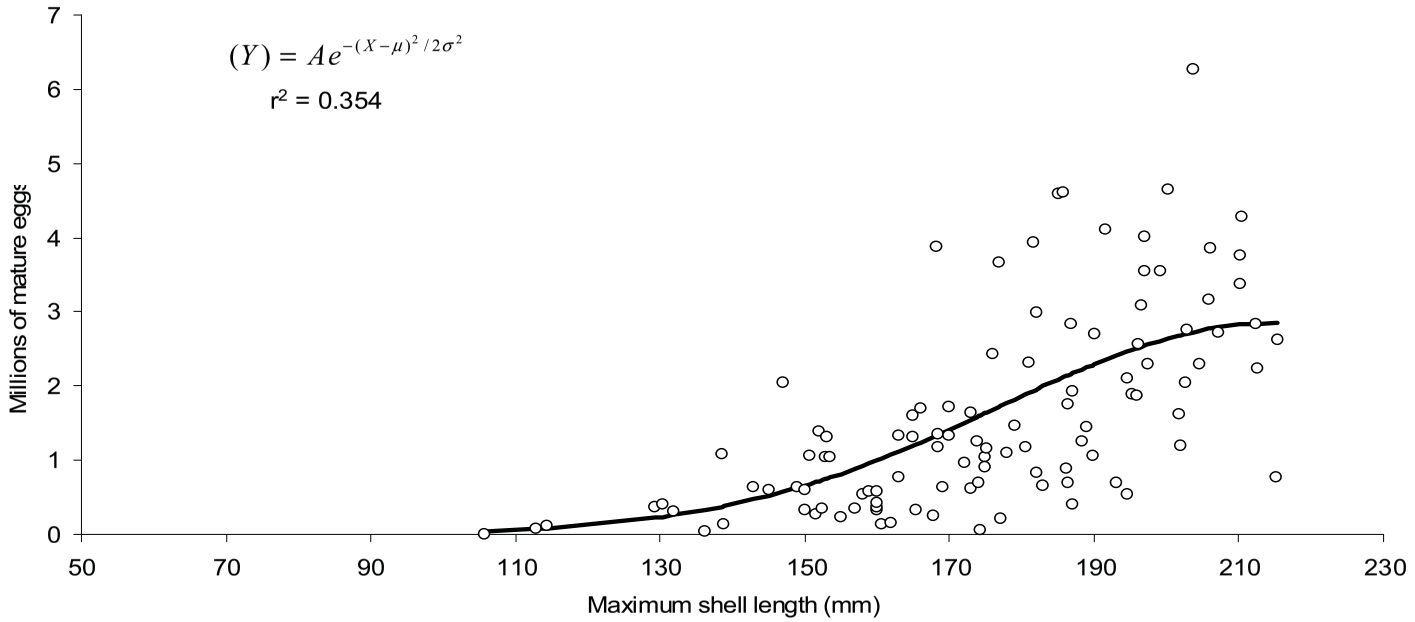

Figure 2. Size specific egg production of red abalone from Rogers-Bennett et al. (2004) with Gaussian curve regression used to determine fecundity values for the projection matrix.

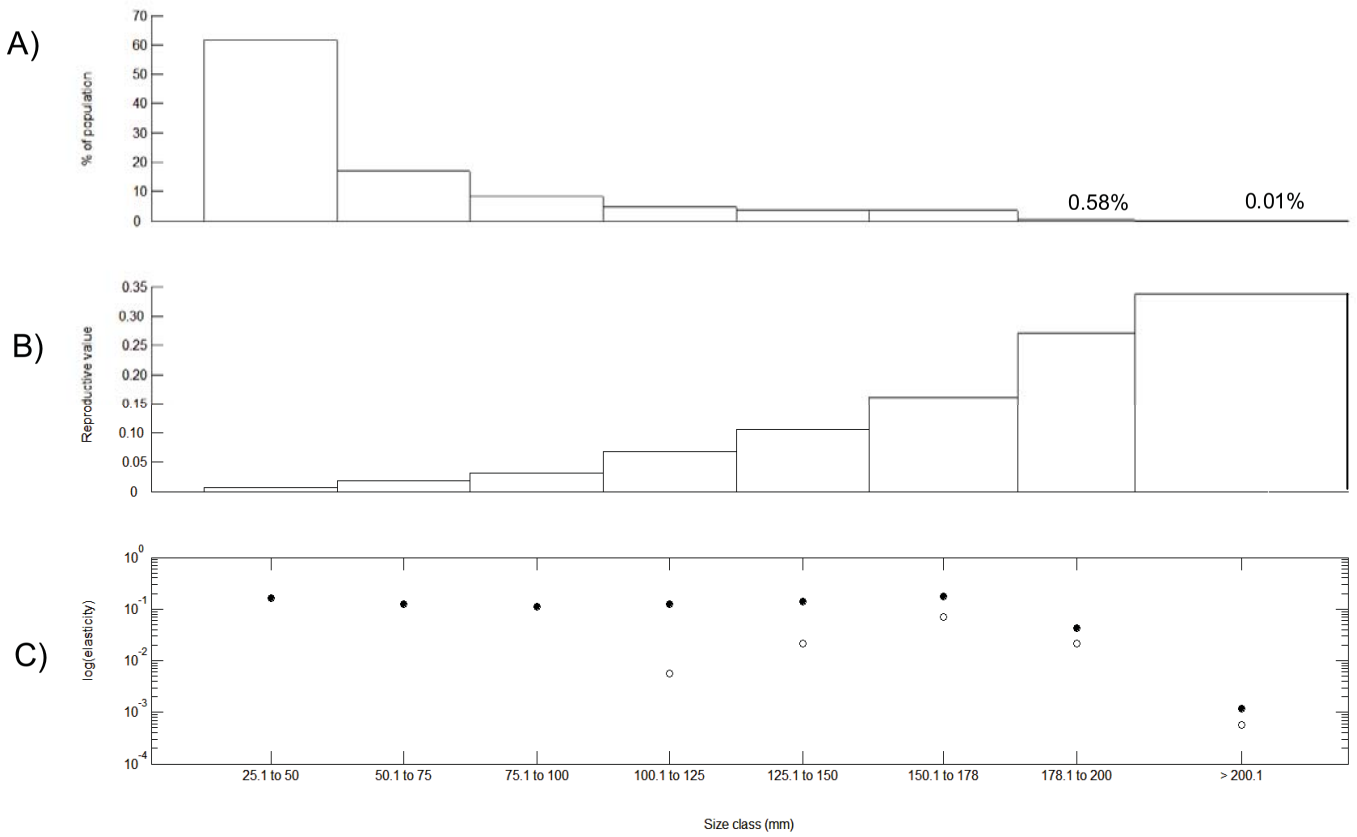

Figure 3. A) Stable size distribution derived from projection matrix (note percents of population given for the largest two size classes. B) Size class specific reproductive values derived from projection matrix. C) Elasticity values of growth and survivorship (gx x px) (•), and fecundity (fx x p0) (•), note y-axis is log scaled.

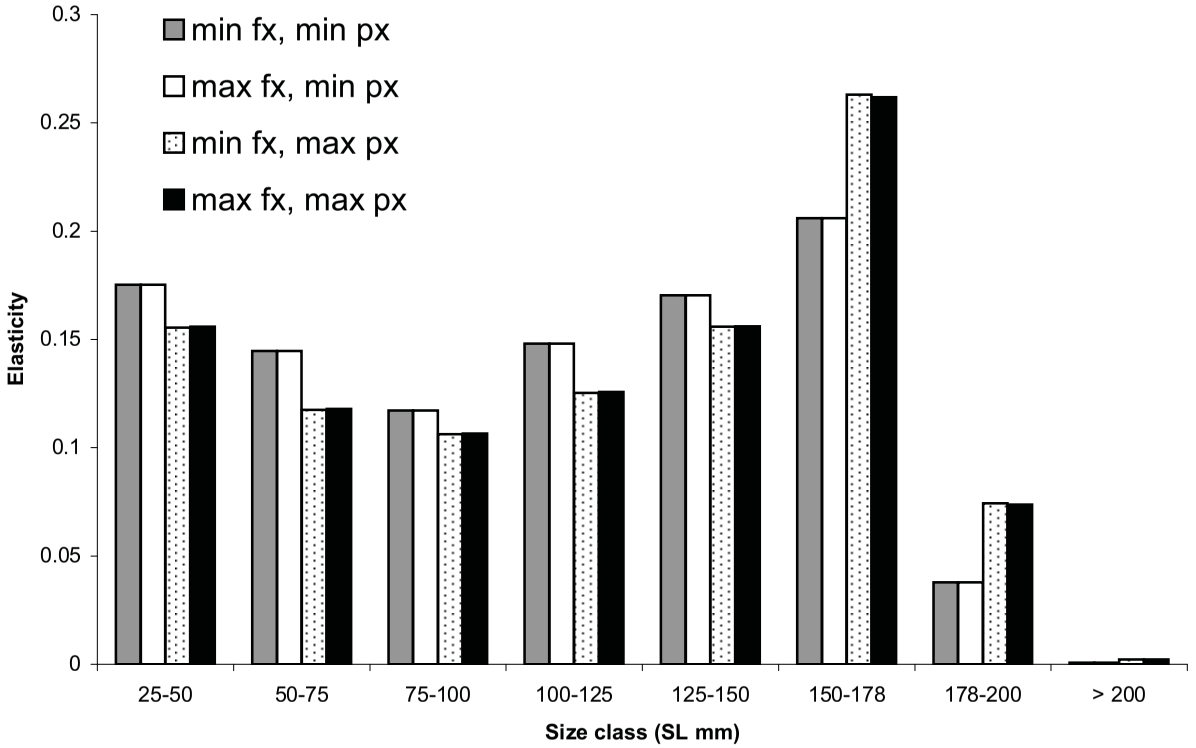

Figure 4. Elasticity results of matrix simulations of alternative vital rates. Min (minimum) values are mean vital rate values minus one standard error of their estimates. Max (maximum) values are mean vital rate estimate plus one standard error of their estimate.

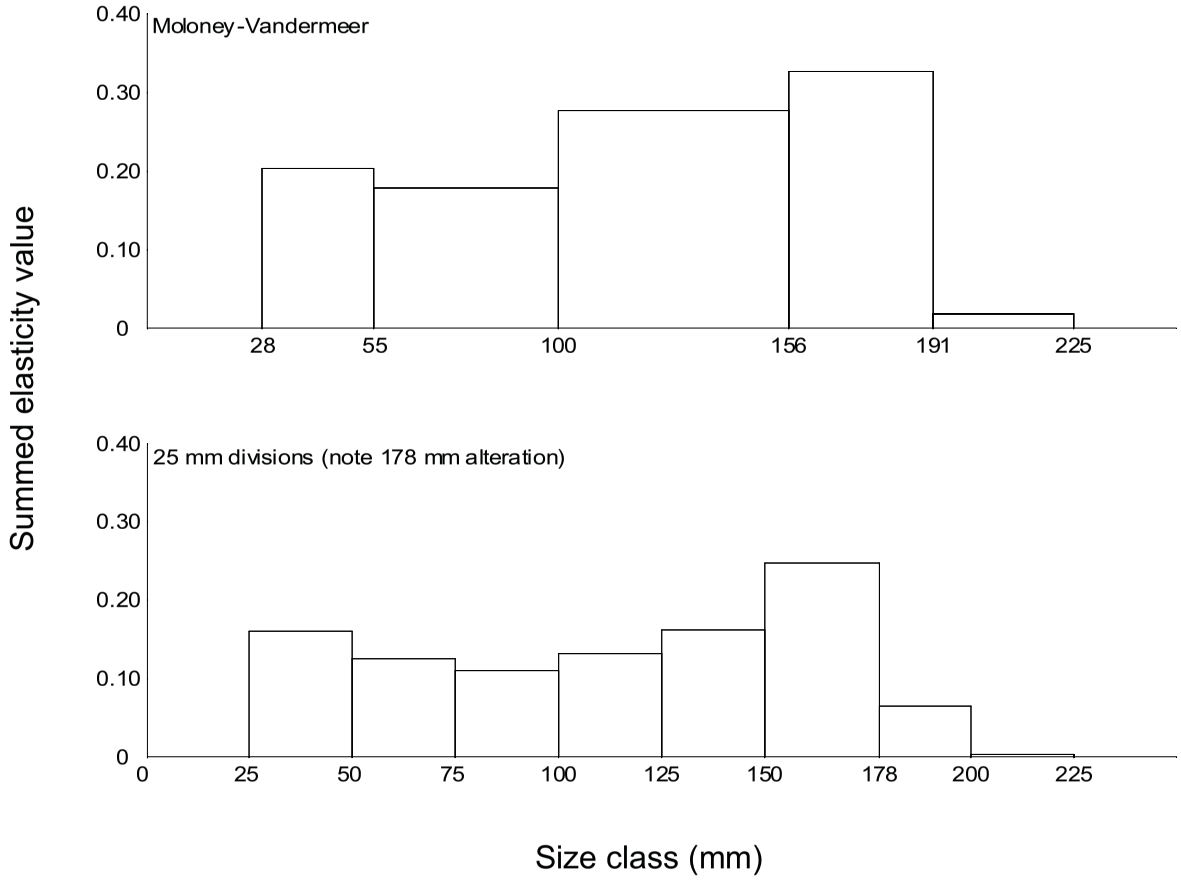

Figure 5. Summed elasticity values for the Moloney-Vandemeer specified size class and 25 mm size class matrices.

CHAPTER 3

Preliminary validation of the age-at-length relationship of red abalone, *Haliotis rufescens*, by analysis of bomb radiocarbon in shell carbonate

ABSTRACT

Current methods to describe age-at-length relationships of red abalone (*Haliotis rufescens*) are insufficient to determine the ages of large individuals because their shell lengths exceed those predicted by model L_∞ values. I evaluated the utility of analyzing atomic bomb generated radioisotope ^{14}C in shell as a method to validate the age-at-length relationship of *H. rufescens*. Fabens' (1965) method was used to determine von Bertalanffy growth function (VBGF) parameters (L_∞ = 313 mm, k = 0.051 y^{-1} (0.042 to 0.059, 95% CI)) based on data from a multi-year, multi-site tag-recapture study. Shell carbonate was sampled at four locations on a single shell (251 mm, maximum shell length (MSL)) with the objective to bracket the rise of the radiocarbon signal, known to occur during ~1957 in the NE Pacific. There was close correspondence to the radiocarbon values of extracted shell carbonate and estimated dates of formation based on VBGF estimates. The 251 mm (MSL) red abalone specimen was predicted to be 27 to 38 years old. This study presents preliminary results from radiocarbon analysis of shell carbonate and demonstrates the utility of validating the age-at-length relationship of red abalone with this method.

INTRODUCTION

Abalone (*Haliotis* spp.) are susceptible to local extirpation by fishing because of slow growth, aggregated near shore distribution, and demand for meat and shells (Sluczanowski 1986, Jamieson 1993, Alvarez-Tinajero *et al.* 2001). Red abalone, *Haliotis rufescens*, support an important recreational fishery in northern California and was once commercially important (Karpov *et al.* 2000). Historically, over-fishing in California of the *Haliotis* spp. complex resulted in reduced abundances and closure of the commercial fishery (Rogers-Bennett *et al.* 2002). These depletions have led to concerns about the sustainability of the recreational fishery. Regulations enacted by the California Department of Fish and Game (CDFG) include gear restrictions, limit recreational fishing to free diving only, regulate annual and daily bag limits, allow take of red abalone only with a minimum size limit of 178 mm maximum shell length (MSL), and prohibit take south of San Francisco Bay (CDFG, Marine Region 2005).

Because red abalone are thought to exhibit asymptotic growth with a maximum recorded size of 313 mm (MSL, maximum shell length) the ages of the largest individuals are unknown, and tag and recapture studies can provide only limited information (Ault 1985, Haaker *et al.* 1998). Current age-at-length estimates from northern California, derived from tag-recapture data, indicate the largest individuals in the population would reach an average maximum size (L_∞) of 170 mm to 236 mm MSL (Ault 1985). Predicted values of L_∞ in southern California range from 182 mm to 212 mm MSL (Haaker *et al.*

1998). These estimates indicate that age and growth determinations may need a more realistic L_{∞} values.

Two alternative strategies for estimating age-at-length are counts of growth zones (discontinuous rings, marks, or lines on the shell) and analysis of seasonal stable isotope patterns in shell carbonate. Growth zones of abalone shells are often very irregular and preclude any form of consistent quantification and annual zones may not be present. (Forster 1967, Poore 1970). The second method of age estimation is the analysis of the ratios of stable isotopes in shell carbonate (Cespuglio *et al.* 1999, Richardson 2000, Gurney *et al.* 2005). Oxygen isotopes, ^{18}O and ^{16}O, are incorporated into shell carbonates in isotopic equilibrium with seawater and can be correlated with temperature, thereby providing a measure of temperature change (Epstein *et al.* 1953). Seasonal patterns in productivity, as evidenced by changes to the isotopic ratios of carbon, ^{13}C and ^{12}C, can also provide a seasonal proxy for shell formation (Fairbanks and Dodge 1979, Krantz et al. 1984, Romanek *et al.* 1987). To detect seasonal patterns of temperature and productivity, carbonate is extracted from the shell along the growth axis. Cyclic patterns observed in the ratios can then provide a temporal basis for growth. Analysis of stable isotopes has proved useful for determining growth rates early in ontogeny when growth rates are highest, but carbonate extraction cannot be performed at the resolution necessary to detect seasonal patterns in older shell material (Romanek *et al.* 1987, L.J. Gurney, University of Tasmania, personal communication). Because of the limitations of these strategies, an independent chronometer for shell carbonate formation is needed for accurate age and growth determination.

The use of the time-specific bomb-radiocarbon (^{14}C) marker preserved in carbonates of organisms is a promising method for validating estimates of age-at-length and longevity (Campana 2001). Atmospheric testing of thermonuclear devices during from 1953 to 1963 doubled the naturally occurring levels of ^{14}C in the atmosphere, and integrated into the oceans and organisms in the mixed layer. Identification of the initial rise in ^{14}C in the skeletal structure of these organisms provides a chronological tool for determining age. In this study, a series of carbonate samples from a single red abalone shell were analyzed for ^{14}C to investigate the feasibility of using the time-specific bomb-radiocarbon (^{14}C) marker to validate the age-at-length relationship and determine growth rates of large abalone; a first attempt to use this technique on abalone.

METHODS

One red abalone shell (251 mm maximum shell length, MSL) was obtained and sampled for ^{14}C. The individual was collected in 1968 ($\pm$ 1 year) near Gualala River, Mendocino, in northern California by Duane Shoemake (Duane Shoemake, 3870 Oakley Road, Antioch, California 94509) , a recreational abalone fisher. Based on the recollection of the fisher the specimen was collected during 1968 ($\pm$ 1 year). To estimate age for the four locations in the shell to be sampled, von Bertalanffy growth function (VBGF) was used as a guide to sample the shell based on tag-recapture data from six sites in northern California (Rogers-Bennett personal communication). Fabens' method was used to derive VBGF estimates (Fabens 1965).

$$L_{recapture} = L_{tag} + (L_{\infty} - L_{tag})(1 - e^{(-k*\Delta t)})$$

In which: 1)$L_{recapture}$ is the MSL (mm) of an individual at the time of recapture; 2) L_{tag} is the MSL (mm) of an individual at the time of tagging; 3) Δt is the duration between the time of tagging and capture, in years; and 4) *k* is the von Bertalanffy rate constant, y^{-1}. The mean estimates and 95% confidence intervals for the rate constant, *k*, were derived using nlinfit, a non-linear curve fitting protocol in MATLAB version 6.5 (The MathWorks 2002). The value of L_{∞} was constrained for curve fitting to the maximum recorded size (313 mm MSL). A Walford plot of the annual change in MSL of 641 individuals that were tagged and recaptured in a 335 to 395 day interval (assumed to represent annual growth) was constructed to estimate *k* for initial nlinfit iteration.

The von Bertalanffy growth function was evaluated qualitatively for goodness of fit to tag and recapture data using the growth vector method of Cailliet *et al.* (1992). Vectors are anchored to the growth curve by assuming that their lengths at first capture correspond to the age predicted by the von Bertalanffy estimates. Vectors of growth, when individuals are at liberty, are drawn based on their horizontal (Δt, years) and vertical (ΔL, mm) components.

Two sources of variability were incorporated into the estimate of date of shell formation at a given shell length. The first source of uncertainty is the date of collection (1968 $\pm$ 1 year). The second source of uncertainty was the 95% confidence intervals for the growth constant (*k*). Estimated dates of shell formation were calculated to incorporate both of these sources of variability. The dates of shell formation at a given length were calculated for a minimum date: A small *k* value (mean value of *k* – 95% CI) and a date of

collection assumed to be 1967 and a large value of k (mean value of k + 95% CI) and a date of collection assumed to be 1969. The mean date of shell formation at a given length was estimated using the mean value of k and the median estimate of the date of collection, 1968.

To obtain carbonate samples for ^{14}C analyses, the shell was sectioned perpendicular to the growth axis using a diamond bladed saw. Thin sections approximately 2 mm wide were extracted and mounted on slides with Cytoseal or wax. Carbonate samples (~5 mg per sample) were extracted from the prismatic layer in the mounted thin sections using a New Wave® micromill. The first sample was taken at the margin of the abalone shell, 251 mm (MSL) for which the date of formation was known (1968 $\pm$ 1 year). Three additional samples were taken at 227 mm, 217 mm, and 75 mm (MSL).

In preparation for radiocarbon analysis, the work area at Moss Landing Marine Laboratories and the shell were tested for potential radiocarbon contamination. Glass filters were used to sample these areas (2 samples and two blanks). Samples were submitted to the Center for Accelerator Mass Spectrometry (CAMS) at Lawrence Livermore National Laboratory (LLNL) and revealed no radiocarbon contamination. Shell samples were analyzed for radiocarbon, ^{14}C, using accelerator mass spectrometry (AMS). Results from AMS were reported as $\Delta^{14}C$ to enable comparison with other bomb radiocarbon records (Stuiver and Pollach 1983).

RESULTS

The specimen collected in 1968 (± 1 year) is predicted to be 27 to 38 years old (Figure 1). The VBGF, with a constrained L_∞ value of 313 mm, predicted the growth constant *k* to be 0.051 y^{-1} (0.042 to 0.059, 95% CI) (Figure 1). This value is less than half of the Walford plot predicted *k* value of 0.123 y^{-1}. The mean von Bertalanffy growth estimate has a poor fit when analyzed with growth vector data. The distribution of growth vectors indicate that the VBGF underestimates growth of small individuals < 160 mm and overestimates growth of individuals larger than this size. The distribution of growth vectors for median sized individuals (~150 mm MSL) is relatively evenly distributed in relation to the estimated mean growth estimates.

The back-calculated dates of shell formation based on the VBGF had the greatest range estimate for the 75 mm MSL than for the carbonate extracted at 217 mm MSL and 227 mm MSL (Figure 2). Shell carbonate removed from the shell when the abalone was 75 mm (MSL) had an estimated date of formation of 1941 (1935 to 1946, 95% CI). Shell carbonate removed from the shell when the abalone was 217 mm (MSL) and 227 mm (MSL) had estimated mean dates of formation of 1959 (1956 to 1962, 95% CI) and 1961 (1959 to 1963, 95% CI). Shell carbonate removed from the margin of the abalone shell would have been formed close to or during 1968 (± 1 year).

There was a close correspondence to the radiocarbon values of extracted shell carbonate and estimated dates of formation based on VBGF estimates to the chronometer of yellow eye rockfish established by Kerr *et al.* (2004) (Figure 3). The back-calculated

dates of formation for the samples taken at 217 mm and 227mm (MSL) may bracket or be the point of the inception of the rise of bomb-derived radiocarbon in this specimen.

DISCUSSION

The value of the growth constant *k* in this study was much lower than previously recorded for red abalone in northern or southern California. Ault (1985), using red abalone collected in northern California and maintained in aquaria, predicted *k* values of 0.11 y^{-1} to 0.19 y^{-1}. Haaker *et al.* (1998) reported growth constant values for tag and recaptured individuals in southern California of 0.12 y^{-1} to 0.27 y^{-1}. The difference in estimated growth rate predicted in this study and previous studies is a result of constraining the value of L_∞. Although the widespread use of the von Bertalanffy curve allows experimenters to compare growth rates among populations and species, the co-variation of *k* to L_∞ may limit the utility of this curve to describe growth of some organisms. The poor fit of the von Bertalanffy curve observed in this study for small abalone has been reported (Matsuishi *et al.* 1995, Troynikov *et al.* 1998). Ebert and Southon (2004) have used the Tanaka curve to model red sea urchin, *Strongylocentrotus franciscanus* growth. Red sea urchin may have a life history similar to red abalone in that both exhibit large juvenile growth rates and red abalone, like red sea urchin, may be long lived. The best model to describe growth is one in which the incorporation of a realistic fixed L_∞ value does not necessarily estimate slow juvenile growth when fit to data. Additionally the predicted L_∞ value should reflect the sizes obtained by individuals observed in the population.

Although the von Bertalanffy curve may not be optimal to describe abalone growth, the correspondence of the radiocarbon concentration and estimated date of carbonate formation for each of the samples corresponds well to the yelloweye rockfish chronometer established by Kerr *et al.* (2004). The effect of the poor fit of the von Bertalanffy growth curve, as indicated by the growth vectors, does result in greater heterogeneity in the estimated date of formation for each of the carbonate samples. The 75 mm had a large range of values for the estimated date of formation but was informative because its radiocarbon concentration is in the range of background pre-bomb values validating its date of formation before 1957. The radiocarbon concentration of the sample taken when the specimen was collected (1968 $\pm$ 1 year) records the elevated radiocarbon concentration in surface waters after 1957 in the NE Pacific. Because of the variability in the estimated date of formation and the few number of carbonate samples taken it is not possible to determine whether either of the 217 mm or 227 mm MSL carbonate samples reflects the inception of the rise in radiocarbon concentration.

Although increasing the number of samples taken from this individual may decrease the error associated in locating the inception of the radiocarbon rise in shell carbonate for this single individual, abalone growth is spatially and temporally variable (McShane and Naylor 1995, Haaker *et al.* 1998). Differences in abalone growth and morphology may be due to local wave exposure and food availability as well as temperature (Leighton 1974, McShane and Naylor 1995, David Ebert, MLML, personal communication). Parameters to describe growth are therefore expected to be heterogeneous for red abalone not only as a result of the ageing method but also individual

variations in growth. It would be desirable to pursue a regional approach to quantify growth for red abalone to enable geographic comparisons and describe local variability in growth rates.

The application of the radiometric carbon method for validation of growth parameters has not been performed for many species of mollusc (but see Turekian *et al.* 1982). The requirements for this technique are known dates of collection, lifetimes that coincide with initiation of the rise of the "local" ^{14}C pulse, and a regional reference series of ^{14}C values. For species that are not long lived these requirements may be prohibitive. Red abalone, based on incidental re-capture, were previously known to live at least 16 years in the wild (Taniguchi and Haaker 1996) and therefore large individuals obtained in the 1970's and 1980's are useful candidates for age validation using the radiometric technique.

These preliminary results indicate that the analysis of radiocarbon concentrations in red abalone shell carbonate can be used to validate the age-at-length relationship of red abalone. A sampling strategy that enables determination of growth rates of all sized individuals, using specimens with known dates of collection and isolating the inception of the rise of radiocarbon in shell carbonate is recommended. Although tag-recapture work has been performed for red abalone, the analysis of radiocarbon concentrations allows determination of growth rates of large individuals, a necessary step to population management.

LITERATURE CITED

Alvarez-Tinajero, M.D.C., Caceres-Martinez, J., and J.G. Gonzalez-Aviles. 2001. Shell boring clams in the blue abalone *Haliotis fulgens* and the yellow abalone *Haliotis corrugata* from Baja California, Mexico. Journal of Shellfish Research 20(2): 889-893.

Ault, J.S. 1985. Some quantitative aspects of reproduction and growth of the red abalone, *Haliotis rufescens* Swainson. Journal of theWorld Mariculture Society 16: 398-425.

Beamish, R. J. and G. A. McFarlane. 1983. The forgotten requirement for age validation in fisheries biology. Transaction of the American Fisheries Society 112: 735-743.

Cailliet, G. M., H. F. Mollet, G. G. Pittenger, D. Bedford, and L. J. Natanson. 1992. Growth and demography of the pacific angel shark (*Squatina californica*), based upon tag returns off California. Australian Journal of Marine and Freshwater Research 43:1313-30.

California Department of Fish and Game, Marine Region. 2005. Abalone Recovery and Management Plan. 359 pages. www.dfg.ca.gov/mrd/armp/entire.html

Campana, S.E. 2001. Accuracy, precision and quality control in age determination, including a review of the use and abuse of age validation methods. Journal of Fish Biology 59: 197-242.

Cespuglio, G., Piccinetti, C., and A. Longinelli. 1999. Oxygen and carbon isotope profiles from *Nassa mutabilis* shells (Gastropoda): Accretion rates and biological behaviour. Marine Biology 135: 627-634.

Ebert, T.A. and J.R. Southon. 2004. Red sea urchins (Stronglyocentrotus franciscanus) can live over 100 years: confirmation with A-bomb ^{14}carbon. Fishery Bulletin 101(4): 915-922.

Epstein, S., Buchbaum, R., Lowenstam, H.A., and H.C. Urey. 1953. Revised carbonate-water isotopic temperature scale. Bulletin of the Geological Society of America 64: 1316-1326.

Fabens, A.J. 1965. Properties and fitting of the von Bertalanffy growth curve. Growth 29: 265-289.

Fairbanks, R.G. and R.E. Dodge. 1979. Annual periodicity of the $^{18}O/^{16}O$ and $^{13}C/^{12}C$ ratios in the coral *Montastrea annularis*. Geochimica et Cosmochimica Acta 43: 1009-1020.

Forster, G.R. 1967. The growth of *Haliotis tuberculata*: Results of tagging experiments in Guernsey 1963-65. Journal of the Marine Biological Association of the U.K. 47: 287-300.

Guerney, L.J., Mundy, C. and M.C. Porteus. 2005. Determining age and growth of abalone using stable oxygen isotopes: a tool for fisheries management. Fisheries Reseach 72:353-360.

Haaker, P.L., Parker, D.O., Barsky, K.C., and Chun, C.S.Y. 1998. Growth of red abalone, *Haliotis rufescens* (Swainson) at Johnsons Lee, Santa Rosa Island, California. Journal of Shellfish Research 17(3):747-753.

Jamieson, G. S. 1993. Marine invertebrate conservation: evaluation of fisheries over-exploitation concerns. American Zoologist 33: 551-567.

Karpov, K. A., P. L. Haaker, I. K. Taniguchi, and L. Rogers-Bennett. 2000. Serial depletion and the collapse of the California abalone fishery. In: Workshop on rebuilding abalone stocks in British Columbia, A. Campbell, ed. Canadian Special Publication of Fisheries and Aquatic Sciences 130:11–24.

Kerr, L.A., Andrews, A.H., Frantz, B.R., Coale, K.H., Brown, T.A. and G.M., Cailliet. 2004. Radiocarbon in otoliths of yelloweye rockfish (*Sebastes ruberrimus*): A reference time series for the coastal waters of southeast Alaska. Canadian Journal of Fisheries and Aquatic Science 61(3): 443-451.

Krantz, D.E., Jones, D.S., and D.F. Williams. 1984. Growth rates of the sea scallop, *Placopecten magellanicus*, determined from the $^{18}O/^{16}O$ record in shell calcite. Biological Bulletin 167: 186-199.

Leighton, D.L. 1973. The influence of temperature on larval and juvenile growth in three species of southern California abalones. Fishery Bulletin 72(4): 1137-1145.

The MathWorks, MATLAB, version 6.5. 2002.

Matsuishi, T., Saito, K., and Y. Kanno (1995). Growth curve of abalone. Bulletin of the Faculty of Fisheries Hokkaido University 46(3): 53-62.

McShane, P.E. and Naylor, J.R. 1995. Small scale spatial variation in growth, size at maturity, and yield- and egg-per-recruit relations in the New Zealand abalone *H. iris*. New Zealand Journal of Marine and Freshwater Research 29:603-612.

Poore, G.C. 1972. Ecology of New Zealand abalones, Haliotis species (Mollusca: Gastropoda) 3. Growth. New Zealand Journal of Marine and Freshwater Research 6(4): 534-559.

Richardson, C.A. 2000. Molluscs as archives of environmental change. Oceanography and Maine Biology: An annual review 39: 103-164.

Rogers-Bennett, L., Haaker, P.L., Huff, T.O., and P.K. Dayton, 2002. Estimating baseline abundances of abalone in California for restoration. CalCOFI Reports 43: 97-111.

Rogers-Bennett, L., Rogers, D.W., and S. Schultz. in preparation. Estimating growth and mortality parameters for red abalone (*Haliotis rufescens*) in northern California.

Romanek, C.S., Jones, D.S., Williams, D.F., Krantz, D.E., and R. Radtke. 1987. Stable isotopic investigation of physiological and environmental changes recorded in shell carbonate from the giant clam *Tridacna maxima*. Marine Biology 94: 385-393.

Sluczanowski, P.R. 1986. A disaggregate model for sedentary stocks: The case of south Australian abalone. In: G.S. Jamieson, and N. Bourne (eds.) North Pacific workshop on stock assessment and management of invertebrates. Canadian Special Publication of Fisheries and Aquatic Sciences 92, p. 393-401.

Stuiver, M., and H.A. Polach. 1977. Discussion: reporting of ^{14}C data. Radiocarbon 19: 355-363.

Taniguch, I.K. and P.L. Haaker. A red abalone tag return after 16 years at liberty. California Department of Fish and Game 82(3): 141-143.

Turekian, K.K., Cochran, J.K., and Nozaki, Y. 1982. Determination of shell deposition rates of *Artica islandica* from the New York Bight using natural ^{228}Ra and ^{228}Th and bomb-produced ^{14}C. Limnology and Oceanography 27(4): 737-741.

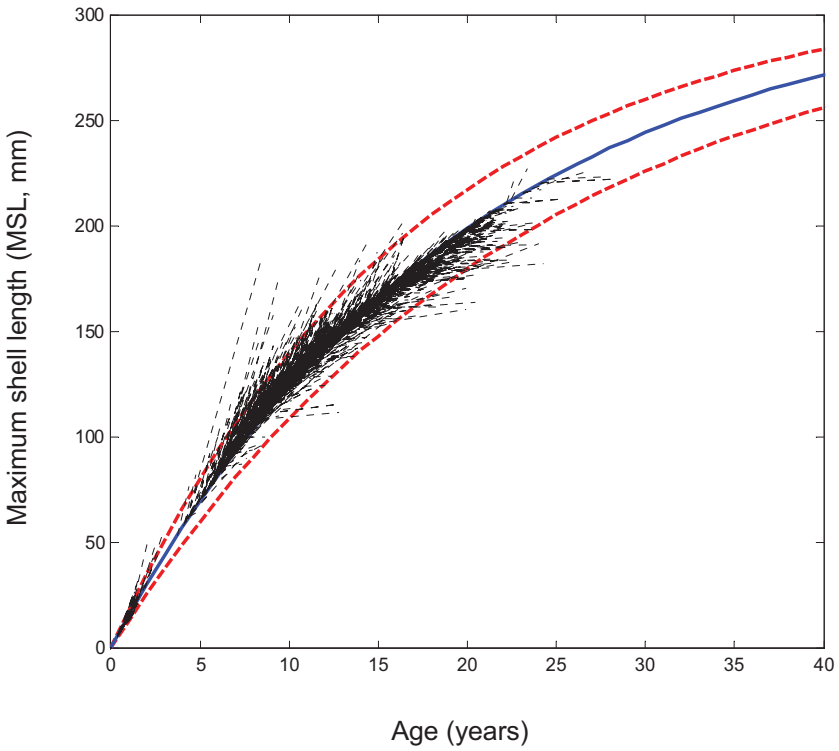

Figure 1. The von Bertalanffy growth curve (solid) with 95% confidence intervals (dashed). The short lines are growth vectors of tagged and recaptured red abalone following the method originally presented by Cailliet et al. (1992). The initial age estimate is the predicted age based on the von Bertalanffy function for the size at tagging which provides the anchor point to the von Bertalanffy growth curve.

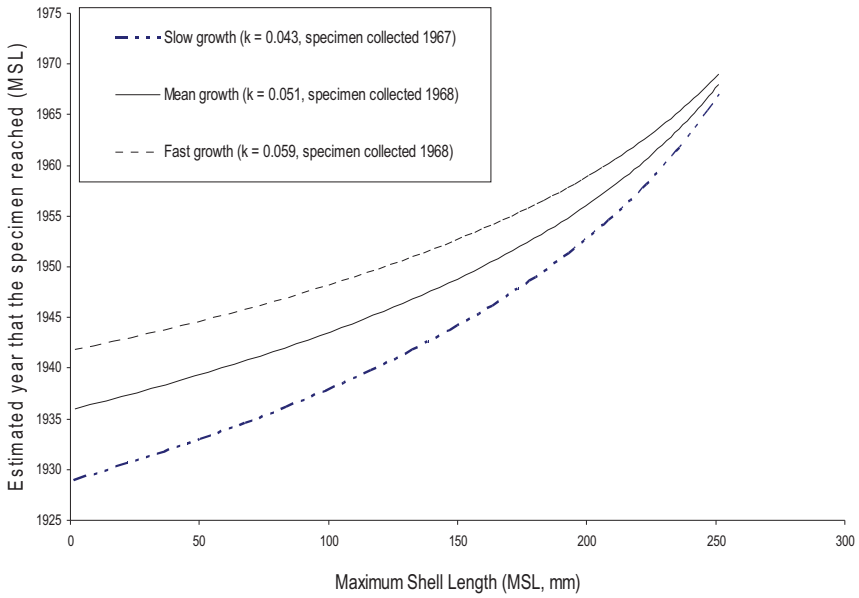

Figure 2. Estimated date of that the specimen reached its MSL based on 'slow', 'mean', and 'fast' growth as derived from von Bertalanffy parameters.

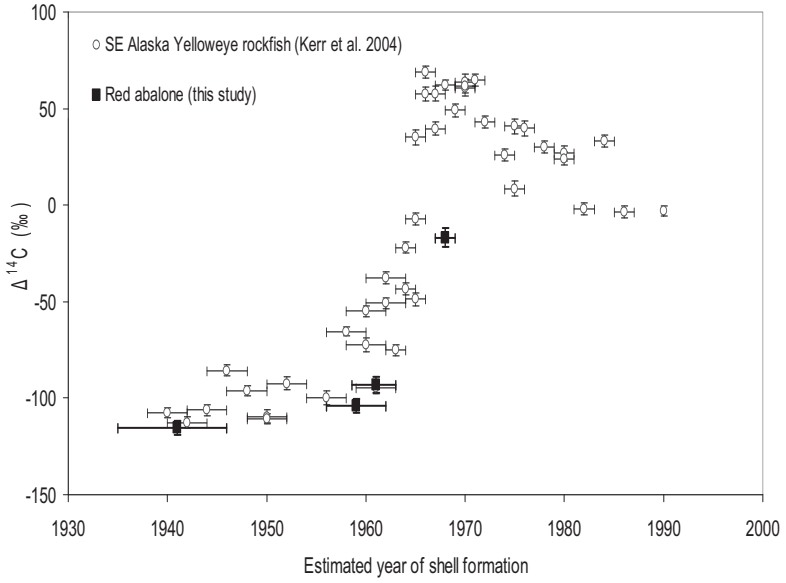

Figure 3. Radiocarbon data, $\Delta^{14}C$, from yelloweye rockfish (Kerr *et al.* 2004) and one red abalone in relation to their estimated dates formation. Vertical error bars represent accelerator mass spectrometry analytical error. Horizontal error bars of Yelloweye rockfish represent uncertainty associated with age determination from growth zones and those of red abalone represent uncertainty in the date of formation as derived from von Bertalanffy estimates.